Dual Effect of CB1R Antagonist on Motor and Psychological Behaviors in 6OHDA-Induced Parkinsonism Model: Probable Role of Ih Currents

Monavareh Soti
Kerman University of Medical Sciences
Hoda Ranjbar
Kerman University of Medical Sciences
Kristi A. Kohlmeier
University of Copenhagen
Moazamehosadat Razavinasab
Kerman University of Medical Sciences
Yaser Masoumi-Ardakani
Kerman University of Medical Sciences
Mohammad Shabani (shabanimoh@yahoo.com)
Kerman University of Medical Sciences

Research Article

Keywords: Parkinsonism model, Ih currents, Cannabinoid, VTA, AM251

Posted Date: January 20th, 2022

DOI: https://doi.org/10.21203/rs.3.rs-1235620/v1

Abstract

Based on data from our lab and others, the endocannabinoid system (ECB_S) appears to be involved in PD-related processes. Therefore, we compared the motor and non-motor effects of the cannabinoid receptor type 1 (CB1R) WIN 55,212-2 (WIN) and selective antagonist (AM251), on motor and non-motor symptoms (NMS) of PD in a mice model generated by an intracerebroventricular (i.c.v.) injection of 6-hydroxydopamine (6-OHDA). To provide further knowledge about the link of CB1R with hyperpolarization-activated current (Ih), we conducted *ex vivo* investigations in the ventral tegmental area (VTA). In the current study, pharmacological blockage of CB1R ameliorated explorative behaviors, balance, muscle strength, and passive avoidance memory deficits induced by 6-OHDA, however, anxious, and depressive-like behaviors were heightened. 6-OHDA exposure induced severe alterations in the spontaneous and evoked firing behavior of DA neurons as evidenced by a significant increase in the mean number of spikes and a decrease in half-width, respectively. Interestingly, an increase in the amplitude of the sag voltage and in the amplitude of the steady state Ih currents was seen. WIN exacerbated 6-OHDA-induced actions by further reducing the spike half-width and increasing the firing frequency, as well as increasing sEPSP amplitudes. The effects of 6-OHDA on sag voltage, Ih currents amplitude, and firing frequency were reversed by administration of AM251. These results suggest that ECBs might underlie some of the 6-OHDA-induced electrophysiological alterations in VTA DA neurons in this animal model of PD and antagonist of this receptor could be effective in modulating the devastating effects of 6-OHDA.

Highlights

- 6-OHDA exposure induced severe alterations in firing behavior of DA neurons
- Blockage of CB1R ameliorated the motor and cognitive deficits induced by 6-OHDA
- 6-OHDA exposure increased VTA neurons excitability
- 6-OHDA induced alterations on Ih currents and firing frequency reversed by AM251

1. Introduction

Parkinson's disease (PD) is the second most common progressive neurodegenerative disorder after Alzheimer's disease [1]. PD is associated with profound [2] and includes akinesia, tremor, rigidity, and postural instability. Besides motor symptoms, non-motor symptoms (NMS) such as cognitive problems and depression are present and likely originate from changes occurring outside the nigrostriatal system. Although NMS are key determinants for the quality of life [3], they remained undiagnosed in over 40% of PD patients [4]. The cause of PD is multifactorial but a role for the gradual loss of melanin-containing nigral neurons in the basal ganglia (BG) leading to unusual dopamine (DA) transmission has been established [5]. A novel finding proposes the aberrant tonic inhibition of the remaining DA neurons through GABA release by reactive glia further promotes PD in animal models [6]. There are several pharmacotherapy options available for PD, including L-DOPA (levodopa) [7], and DA D2-receptor agonists [8], but long-term use of these compounds is limited by the development of side effects, including abnormal

involuntary movements (dyskinesia) [9]. Regardless, DA-based therapies have a limited effect on cognitive deficits in PD [10,11] and development of more effective and tolerable treatments are imperative. As the neurophysiological actions of endogenous cannabinoids are mediated mainly by one of the two known cannabinoid receptors, the type 1 (CB1R), and the CB1R plays a role in activity of DA neurons [12,13], one of the treatment options proposed in recent years is to exploit the endocannabinoid system (ECBs) with the use of CB1R modulators [5].

The CB1R is by far the most common G-protein-coupled receptor and is highly concentrated in the BG [14–16]. However, the results of studies with various models of experimental PD that have examined the effects of both agonists and antagonists of CB1R alone or as co-adjutants are controversial. Plant, synthetic and endogenous cannabinoids have been reported to have inhibitory effects on motor activity in both humans [17] and experimental animals [18]. Numerous studies have shown that CB1R agonists and CB1R modulators improve motor functions [19–21], however, a growing body of evidence from animal models and human studies has shown that CB1R agonists have complex effects on cognitive functions such as attention, learning, emotional reactivity, Improvement of sensory perception and impairment or improvement of short term memory [22–25]. In the passive avoidance learning (PAL) task, CB1R activation reversed opioid-induced memory impairment [26] but this activation has been shown to affect PAL in other reports [27,28]. Several CB1R-mediated signaling pathways have been identified, one of which is via the hyperpolarization-activated cyclic nucleotide-gated (HCN1-4) channels that underlie the hyperpolarization-activated current (Ih) [29].

Ih is a mixed cationic current carried by Na^+ and K^+ activated by hyperpolarizing voltage steps to potentials that are more negative than the resting potential of cells [30]. Ih currents play an important role in controlling rhythmic activity in neural circuits [31,32], determination of the resting membrane potential [33,34], dendritic integration [35,36] and synaptic transmission [37,38]. Evidence has linked CB1R-mediated long-term potentiation (LTP) in the hippocampus to Ih [29]. Because of their role, defective HCN channels are natural candidates in the search for possible causes of neurological disorders in humans. HCN channels are also present in the midbrain system, where they finely regulate the activity of DA neurons. HCN2 and HCN4 channels are strongly expressed in DA neurons of the midbrain, where they are involved in the regulation of spontaneous network activity [39–42]. Interestingly, a potential role for these channels in the pathogenesis of PD has recently emerged [43].

As a first aim, the present study used a combination of molecular and behavioral approaches to investigate the effect of the CB1R agonist, WIN 55,212-2 (WIN), and the antagonist, AM251 (AM) on motor and NMS, in a mouse Parkinsonism model in which the DA midbrain neurons have been lesioned. In a second aim, as activity of the midbrain DA neurons are critical in cognitive and depressive-like behaviors, and activity of these cells has been shown to be controlled by CB1Rs and Ih, we investigated the effects of 6-OHDA and the CB1R agonist and antagonists on Ih currents and sag voltage in midbrain DA neurons in the ventral tegmental area (VTA).

2. Results

2.1. Sucrose intake

Administration of 6-OHDA decreased (26%) sucrose intake as compared to the intake seen in the DMSO group. However, administration of 3 different concentrations of WIN resulted in an increase of sucrose intake (7.5 nmol: 10%, 750 nmol: 17%, and 75 µmol: 7%) while a relative reduction was observed in AM-treated groups (20 nmol: 14%, 2µmol: 8%, and 200 µmol: 12%). The same pattern was repeated in the PD group, treatment with WIN increased sucrose intake (7.5 nmol: %13, 750 nmol: %6, and 75 µmol: %7) and AM decreased (20 nmol: %3, 2µmol: %7, and 200 µmol: %16) it in 6-OHDA-lesione mice during 3 days compared to DMSO group.

2.2. 6-OHDA-induced tail suspension impairment was not reversed by AM251

The TST is a preclinical test with good predictive validity that is widely used to detect antidepressant-like activity [44], and the ability of a drug to reduce the time a mouse spends immobile has been used to define antidepressant-like activity. As expected, the 6-OHDA group showed a significant increase in immobility time compared to that seen in the DMSO ($P < 0.05$). However, the 6-OHDA+ WIN treatment group did not exhibit a significantly different immobile time when compared to that seen in the DMSO group. AM administration in 6-OHDA-lesioned mice significantly increased immobility time compared to that seen in the DMSO group when similarly exposed to the CB1R antagonist (20 nmol, 2µmol: $P < 0.005$ and 200µmol: $P < 0.001$) (Fig. 2).

2.3. 6-OHDA-induced explorative deficiency was reduced by AM251

Several studies have reported that 6-OHDA induces an up-regulation of CB1R in the BG [45,46], which is exacerbated when the DA injury is high. It has been shown that the CB1R displays a reduced pattern during early-stage of PD [47]. In our studies, the bilateral injections of 6-OHDA into the lateral ventricles produced hypokinetic signs of PD at 1 week post-injection. Based on this, we surmise that our model likely causes a moderate lesion, which mimics the first phases of motor disability of human PD, which could be the phase most sensitive to effects of CB1R manipulation. Therefore, we investigated the effect of different degrees of stimulation and blockade of CB1R on PD motor symptoms during this period. Mice of the 6-OHDA and 6-OHDA + WIN groups exhibited a decrease in total distance moved (TDM) ($P < 0.01$), velocity ($P < 0.001$), and mobility ($P < 0.05$) when compared to values for these same parameters in the DMSO group (Fig. 3A-C). A positive effect of the high concentration of AM (200µmol) upon TDM ($P < 0.05$), and velocity ($P < 0.01$) was noted in the PD group. When comparisons were conducted between groups for measures of rearing frequency, grooming frequency, and time spent in the central zone which is used to evaluate anxiety like behavior, the 6-OHDA and 6-OHDA + AM (200µmol) groups spent less time in the central zone compared to the DMSO group ($P < 0.01$, Fig. 3D). 6-OHDA + WIN, (7.5µmol) resulted in

a decrease in rearing frequency compared to WIN administration in the DMSO group ($P < 0.05$, Fig. 3E). Pretreatment with CB1R agonist/antagonist had no effects on grooming frequency as compared to the other groups (Fig. 3F).

2.4. 6-OHDA-induced balance and muscle strength disturbances were ameliorated by AM251

Recorded across three sequential trials, 6-OHDA ($p < 0.001$) and 6-OHDA + WIN ($p < 0.001$) treated animals showed a decrease in time of falling as compared to the DMSO groups in the wire and rotarod test. Interestingly, mice treated with the CB1R selective antagonist exhibited an increased duration on the wire and rod at all concentrations utilized (20 nmol $P < 0.05$, 2 µmol $P < 0.01$, 200 µmol: $P < 0.001$) in comparison to the 6-OHDA treated group (Fig. 4A, B).

2.5. 6-OHDA-induced impairment of performance in the passive avoidance test was partially reversed by AM251

Shock number in WIN groups (750nmol, 75µmol) increased compare to control in the PAL task ($P < 0.001$, Fig. 5A). In the retention trials, which were performed 24h later, the STL of 6-OHDA treated mice exposed to different concentrations of WIN (7.5 nmol $P < 0.05$, 750 nmol $P < 0.01$, 75µmol $P < 0.001$, Fig. 5B) were significantly shorter than that seen in DMSO animals. Comparison of TDC values also showed a significant increase in 6-OHDA+WIN groups (750 nmol $P < 0.001$, 75µmol: $P < 0.001$, Fig. 5C) compared to DMSO. AM251 decreased shock number ($P < 0.01$) and TDC ($P < 0.05$) consistent with raising STL (20 nmol $P < 0.01$, 2 and 200 µmol $P < 0.05$) compared to 6-OHDA group. The greater number of shocks required for learning in the 6-OHDA mice treated with the CB1R agonist suggested deficits in learning. However, the learning deficits were significantly compensated by a low dose of AM251.

2.6 6-OHDA injection reduced TH activity and TAC; AM251 reversed the effect on TH but not TAC

As shown in figure 6, 6-OHDA treated mice exhibited a significantly lower level of TH activity (pg/ml) in the midbrain, when compared to that seen in the DMSO group ($P<0.01$). The exposure of DA VTA neurons to the cannabinoid antagonist, AM251, was effective in reducing the 6-OHDA-induced TH activity deficit as treatment with AM (200µmol) was not associated with a significant decrease in TH activity following 6-OHDA lesion. As expected, 6-OHDA exposure triggered oxidative stress as indicated by a significant reduction of total antioxidant capacity (TAC). However, there was no statistically significant difference between WIN and the AM treated groups regarding TAC (pg/ml) in the midbrain.

2.7. CB1R agonist/antagonists had no effect on the passive membrane properties of VTA neurons

There were no statistical differences seen between the treatment groups of membrane passive properties (rest membrane potential (RMP), axis resistance (Ra) or membrane capacitance (Cm) of VTA DA neurons

indicating that exposure to 6-OHDA whether in the presence or absence of cannabinoid agonist or antagonist had an effect on these parameters (Fig. 7A- C).

2.8 Ih currents, sag voltage and spontaneous activity are increased in VTA 6-OHDA exposed and WIN-exposed neurons

In CB1R agonist/antagonist and 6-OHDA-exposed slices, a total of 59 VTA neurons were recorded, of which 36 (61%) were putatively DA containing based on the well-established criteria of presence of Ih elicited by negative current or voltage steps. Of the recorded neurons, 44.4% were spontaneously active. Presence of Ih was evaluated by I-V (current versus voltage) curves (Figs. 8 and 9A, B), and elicitation of a 'sag' voltage in response to negative current injection and cells positive for Ih were included in the electrophysiological analysis. In total, 59 cells were examined and 36 cells showed electrophysiological properties of DA cells. The passive and active properties of 6 cells were examined for each group.

Analysis of I-V curves in voltage clamp mode (Fig. 8) showed that the amplitude of Ih currents were significantly greater in 6-OHDA and 6-OHDA+WIN (2 μM) treatments compared to control as measured at 120 and 130 mV ($p < 0.05$) as well as at 140 mV ($p < 0.001$). Ih currents activated by hyperpolarizing potentials and our data showed an increased in amplitude of Ih currents close to 1000 pA in 6-OHDA and 6-OHDA+WIN groups compared to control.

Ih currents play an important role in generating a sag voltage, which is a return to a more depolarized state following a hyperpolarization sufficient to activate Ih (Fig. 9A and B). To determine the effects of modulation of CB1R on Ih currents in normal and 6-OHDA treated slices, we studied the sag voltage. 6-OHDA was associated with a significant increase ($P < 0.001$) in the sag voltage after the application of hyperpolarizing current pulses (-100 pA and -500 pA). 6-OHDA alone and in combination with WIN increased sag voltage at -100 pA ($P < 0.001$) compared to control. In 6-OHDA treated slices, AM administration resulted in a reduction in the amount of sag voltage at -100 pA ($P < 0.001$) and -500 pA ($P < 0.005$) when compared to the voltage seen with 6-OHDA alone.

DA neurons from 6-OHDA-exposed mice in the presence of a hyperpolarizing conditioning pulse displayed a significant increase in the number of rebound action potentials and a reduction in the first spike latency at both -100 pA and -500 pA ($P < 0.05$) (Fig. 9C-F). An increased rebound firing rate and a decreased spike latency were observed in DA neurons in the 6-OHDA group, suggesting that Ih is actively involved in the generation of the spontaneous pacemaker activity (Fig. 9C, D). Presence of Ih currents confer spontaneous pacemaker activity (Fig. 10A-C). DA neurons in 6-OHDA-exposed slices and WIN exposed slices demonstrated higher spontaneous firing frequency ($P < 0.05$, Fig. 10A), consistent with the observed smaller half-widths when compared to these same parameters in the control neurons ($P < 0.05$, Fig. 10B). Although 6-OHDA and the CB1R agonist altered the firing frequency and action potential half-width, they did not affect the regularity of DA neurons firing as the interspike intervals were unchanged (Fig. 10C).

For further evaluation of neuronal excitability associated with CB1R agonist/antagonist exposure, input resistance (Fig. 11A) which was calculated from the change in membrane potential evoked by hyperpolarizing current steps, rheobase (Fig. 11B) which is the current required to bring the membrane potential to threshold to fire action potentials, and the firing threshold were measured in response to a depolarizing current ramp from 0 to 1000 pA lasting 1000 ms. VTA DA neurons in 6-OHDA-exposed cells and WIN-exposed cells showed a reduced resistance and a lower rheobase suggestive of a heightened excitability (Fig. 11). 6-OHDA+ AM251 cells showed lower rheobase compare to AM251cells.

The effects of CB1R agonist/antagonist on spontaneous excitatory synaptic activity in DA neurons of exposed to 6-OHDA is illustrated in (Fig. 12). The amplitude of sEPSCs in the DA neurons of the both 6-OHDA ($P < 0.01$) and 6-OHDA+ WIN ($P < 0.001$) was increased which represented a significant difference (Fig. 12A) however, inter event intervals of sEPSCs did not show a significant difference.

3. Discussion

Our behavioral assessments confirmed a positive effect of the highest examined concentration of AM251 (200µmol) upon explorative, balance and muscle strength in PD mice however, 6-OHDA- induced depression and anxiety were intensified by exposure to AM251. 6-OHDA was associated with impaired learning as evaluated by the PAL task and exposure to WIN exacerbated this impairment. However, strikingly, pharmacological inhibition of CB1R activity abolished 6-OHDA-induced PAL deficit. In vivo exposure to 6-OHDA also induced severe changes in the spontaneous and evoked firing behavior of DA neurons, which was demonstrated by a significant increase in the mean number of spikes and a decrease in the half-width. Interestingly, an increase in the amplitude of the sag voltage and the amplitude of the steady-state Ih currents were observed. Consistent with an effect in increasing Ih, WIN exacerbated the 6-OHDA-induced effects by further reducing the spike half-width and increasing the ignition frequency, as well as increasing the sEPSP amplitudes. The effects of 6-OHDA on the sag voltage, the amplitude of the Ih currents and the ignition frequency were reversed by the administration of AM251.

Various animal models have been developed to study the mechanistic underpinnings of PD, and potential therapeutic intervention for this disease. The 6-OHDA animal model in which DA midbrain neurons are lesioned has been widely accepted to study the mechanisms of PD and effectiveness of treatments. 6-OHDA is neurotoxic to DA neurons through mechanisms involving auto-oxidation and increase inflammation biomarkers eventually leads to motor and non-motor impairments such as cognitive deficits like those observed in patients with PD [48–53].

CB1Rs are densely distributed in areas of the brain related to motor control, cognition, emotional responses, motivated behavior, and homeostasis, suggesting a definitive role in these processes [54]. In agreement with this, CB1Rs have been shown to play a pivotal role in the control of movement and pathogenesis of some movement disorders such as PD by modulating GABA, glutamate, DA and other neurotransmitters throughout the BG. Additionally, dysfunctional HCN channels which mediates Ih currents have been suggested to be involved in different experimental models of PD [55,56], and evidence

for a potentially relevant role of Ih currents in the pathogenesis of PD has grown considerably [43]. Our study has attempted to clarify a link between Ih and CB1R in an animal model of PD.

Our results also confirmed that microinjection of 6-OHDA into lateral ventricles produced motor and cognitive deficits in mice that were observed by behavioral assessments. In the open field test, 6-OHDA decreased TDM, velocity and mobile duration. Moreover, when the time spent in the different areas of the apparatus was assessed, 6-OHDA treatment caused a decrease in time spent in the center and a corresponding increase in time spent in the perimeter suggesting that, irrespective of direct effects of 6-OHDA upon motor function, treatment was anxiogenic in mice.

Interestingly, while CB1R agonist ameliorated 6-OHDA-induced deficits in TDM, velocity and mobile duration, it had no effect on anxiogenic effects. Our data are in accordance with previous studies as it has been shown that CB1R antagonist/inverse agonist SR141716A (rimonabant) and AM251 in different PD models (6-OHDA and reserpine-treated rats and MPTP-lesioned marmosets) improve motor performances [57–60]. Moreover, a main non-motor symptom of PD is cognitive decline that predisposes the majority of patients to progression into dementia [61]. Our results also showed that PLA had deteriorated in the mice with 6-OHDA-induced PD and treatment with augmentative dosages of WIN deteriorated PAL while it can compensate by AM251. The data presented here demonstrated that 6-OHDA implication increased depressive-like behavior in tail suspension test in mice, which was reduced by WIN.

Because of key regulatory role of TH in the biosynthesis of catecholamines, it is associated with the pathogenesis of several neurological and psychiatric diseases, including PD. We measured TH activity to ensure the destruction of DA neurons and observed that 6-OHDA caused a dramatic reduction in the TH activity similar to that found by other authors [62,63] concurrent with TAC reduction. In our study, AM251 was found to inhibit 6-OHDA-induced reductions in TH activity; however, there was no statistically significant difference between the AM251 treatment groups regarding TAC level (pg/ml) in the midbrain. It appears that inhibiting the reactive oxygen species (ROS) is not the way AM251 is working; moreover, our result did not reveal alteration in TAC level following administration of CB1R agonist.

The VTA contains a popular (70 percent) of DA cells [64] and the projection fields of these neurons seem to reach the prefrontal cortex and limbic [65], and it is under tonic inhibitory control from the nucleus accumbens (NAc) and ventral pallidum. Medium spiny neurons from the NAc which release GABA, project to the VTA where they can affect GABAergic projection neurons or DA neurons [66]. DA neurons in VTA express Ih currents mediated by HCN channels that have been shown to play a significant role in maintaining membrane potential within the range necessary for the control of neuronal excitability. Based on the cellular distribution and structures of the HCN channels, they may influence neuronal activity. Ih currents have been revealed to mediate excitability in DA neurons and thus can powerfully influence the neuronal activity [67] and blockade of these channels causes a reduction in the neuronal output.

The results showed an over-excitability of VTA-DA neurons in 6-OHDA-treated slices and a plausible role for Ih currents. Meurers et al. (2019) reported an upregulation of HCN3 in the 6-OHDA model of PD, which

was accompanied by an improved rebound excitability of the BG output neurons [68]. HCN3 upregulation has been proposed as a new candidate mechanism leading to in vivo changes in electrical activity in BG output neurons of the Parkinsonian brain. The heightened excitability of VTA-DA neurons could be due to increases in Ih currents through HCN channels [69]. In the current study, 6-OHDA induced robust alterations in the electrophysiological properties of DA-VTA neurons.

In addition, 6-OHDA exposed VTA-DA neurons treated with WIN also exhibited hyperexcitability when compared to electrophysiological recordings conducted in control cells. WIN exposure also caused an increase in inward rectification after hyperpolarization, as evidenced by a significant increase in sag voltage, suggesting that the Ih currents underlying inward rectification were caused by 6-OHDA and CB1R agonist exposure could be changed. The results of several studies showed that cannabinoids can activate an inwardly rectifying K^+ current [70,71], whereas Schweitzer (2000) reported that cannabinoid agonists did not affect the inwardly rectifying cationic Ih currents in the hippocampal CA1 neurons [72].

In contrast to our results, Huang *et al*., reported loss of HCN1 expression in HCN1-null mice and abolishment of Ih lead to enhanced cortical excitability and epileptogenesis. In addition, lack of this channel increased the dendritic input resistance in cortical neurons, which lead to greater synaptic integration, and □ring [73]. Also, inconsistent with our suggestion, genetic and pharmacological animal models of PD have revealed a progressive downregulation of HCN channel activity following DA neuronal loss, without channel protein expression alteration [55]. Interestingly, pacemaking activity and reduced burst spiking were restored via delivery of HCN subunits, but motor impairment induced by DA depletion was not reversed [56]. Computational modeling of globus pallidus (GP) activity supported a role of HCN channel downregulation in PD [74]. Masi *et al*. showed that MPP+ (a potent Parkinsonizing agent) leads to a dose-dependent reduction of spontaneous activity of Ih in substantia nigra pars compacta (SNc) DA neurons, characterized by an increased responsiveness toward synaptic excitation [43].

However, findings of VTA-DA neurons activity in the present study demonstrated a reduction in excitability threshold and higher levels of spontaneous firing with CB1R agonist exposure. The electrical activity of DA cells is essential in regulating the synthesis and release of DA and 6-OHDA exposure-induced alterations in the electrical activity of DA neurons could contribute to altered DA function. In the current study, we also found an increase in spontaneous firing frequency and a decrease in rheobase; both imply a neural hyperexcitability. In this work, our results showed that after the induction of CB1R activation, both the steady state Ih currents amplitudes and sag voltage were increased, implying a hyperexcitability state in VTA-DA neurons. The sEPSC results suggest that presynaptic alterations in glutamate-releasing neurons which terminate on VTA-DA neurons might also play a role in CB1R-associated hyperexcitability and blocking of them might modulate these alterations. These changes might be due to alterations in neural inputs from other neurons, though they must be assessed in the future studies. Additional studies for blocking the Ih currents prior to the motor and depressive-like behavior tests might also demonstrate the role of Ih currents in observed alterations.

Because adult DA neurons do not express CB1R[75], it is possible that WIN may have interacted with inhibitory inputs to the VTA-DA neurons. This claim is further verified by studies reporting that CB1Rs are located mostly on pre-synaptic terminals of GABAergic neurons in the VTA [76], amygdala [77], hippocampus [78], and in the pars reticulata of substantia nigra [79] where they exert inhibitory effects on neurotransmitter release. This indirect inhibition of GABA afferents may clarify the excitatory pro□le detected in VTA neurons observed in the present study.

The role of Ih currents in neural excitability could also explain the overexcitability of VTA-DA neurons and thus offer an opportunity to manipulate them in future studies to determine the effect on locomotor and depressive-like behavior. This increase in excitability observed in DA neurons in this model may be a compensatory mechanism in the remaining neurons that can lead to excitotoxicity. With increasing exposure to 6-OHDA and 6-OHDA + WIN, the number of living neurons decreased.

The changes in 6-OHDA and 6-OHDA + WIN were aimed at increasing the Ih current and excitability. Therefore, this increase in excitability may be partially caused an increase in Ih currents, since one study found that 6-OHDA amplified Ih currents [80]. Consistent with the hypothesis that changes in VTA-DA transmission have a role in WIN-associated. In the behavioral results, we found that VTA-DA neurons in WIN-preserved mice showed overexcitability, as evidenced by the significant increase in ring frequency and the need for a lower current to trigger an action potential. WIN-associated changes in excitability were accompanied by significant increases in Ih flow amplitude and rebound action potentials and a decrease in the action potential half-width and first spike latency. Another reason for the difference in results observed from previous studies may be related to different types of HCN channels. In addition, one of the reasons for the differences in our results may be related to the area of study, so the studies that showed a decrease in Ih were in the GP and the SNc while our focus was on VTA.

In conclusion, the present study demonstrated that CB1R antagonist improves locomotor and memory impairment in the mice 6-OHDA model of PD. However, no changes were seen in antioxidant levels of the Parkinsonism mice treated with antagonist/agonist cannabinoids, despite a decrease in the 6-OHDA group. Considering that current therapy for PD just relieves motor symptoms, we suggest that CB1R modulators may serve as an adjunct therapy for the alleviation of memory deficits in patients with PD. Taken together, findings from the electrophysiological evaluations demonstrated that 6-OHDA and exposure to CB1R agonist resulted in heightened excitability of VTA DA neurons, which could be due in part to increases in Ih currents mediated by HCN channels. Further understanding of the mechanisms by which CB1R activation alters VTA DA neuron excitability may help to postulate therapeutic targets for interventions to reduce negative behavioral outcomes in PD.

4. Materials And Method

4.1. Animals

In the present study we used a mouse model of PD consisted of bilateral injections of 6-OHDA into the lateral ventricles. Male Swiss mice (weighing 25–35g) were purchased from the Kerman University of Medical Sciences and were housed with controlled photoperiod (lights on: 07:00–19:00 h), at 22±1°C with food and water available. The Kerman University of Medical Sciences Ethic Committee *(IR.KMU.REC.1398.012)* approved all the procedures. Animals were habituated to the housing conditions for 2 weeks before the experiments and were handled daily, in order to make them amenable to behavioral testing (Fig. 1). Male mice (n= 9/group) were divided into fifteen groups: control (which did not have surgery and received no injection), sham (underwent surgery and received vehicle (DMSO)), cannabinoid agonist (WIN; 7.5 nmol [81], 750 nmol, and 75 µmol/mouse), cannabinoid antagonist (AM; 20 nmol [81], 2µmol, and 200 µmol/mouse), 6OHDA (40 µg in 2 µl saline containing 0.05% ascorbic acid (to avoid oxidation) [82], 6-OHDA+ cannabinoid agonist and 6-OHDA+ cannabinoid antagonist.

4.2. Surgery and Microinjection

Desipramine (25 mg/kg) was intraperitoneally administered 30 min before injection of 6-OHDA (hydrochloride salt; Sigma, USA), to block noradrenaline reuptake. Mice were anesthetized (ketamine 90 mg/kg + xylazine 10 mg/kg, i.p.) and a stainless steel guide cannula was implanted stereotaxically into the cerebral ventricles at the following coordinates: AP=−0.3 mm, ML=±1.0 mm and DV=−2.5 mm relative to the bregma [83]. 6-OHDA, or the same volume of the vehicle (for sham), was injected into the cerebral ventricles of each mouse [82]. Cannulas were attached to the cranium by dental acrylic cement. After the surgery, animals were allowed 1 week of recovery to modify neurochemical levels, similar or close to DMSO-operated animals. After 1 week recovery and the appearance of negative symptom of Parkinsonism namely the reduction of motor activity, WIN (; Sigma, St. Louis, MO, USA) and AM (; Sigma, St. Louis, MO, USA) were injected into the cerebral ventricles for three consecutive days. Drugs were administered via guide cannula (22-gauge) using injection needle (27-gauge) connected by a polyethylene tube to a 1µl Hamilton micro syringe. The injection needle was inserted 1 mm beyond the tip of the guide cannula. The volume injected was 1.5µl/side with the infusion rate 1µl/min, and then the needle was left in place for 3 min before being slowly withdrawn. This avoids the occurrence of reflux and of a rapid increase in intracranial pressure. 24h after last i.c.v. injection, behavioral testes were assessed. In this lesion model attempted to partial DA denervation of the striatum with a retrograde degeneration of DA cell bodies in the substantia nigra and the mesolimbic DA pathway, closely approximates the neuronal degeneration observed in human idiopathic Parkinson's disease.

5. Behavioral Assessments

5.1. Depressive-like behavior

5.1.1. Sucrose preference test

The anhedonia that occurs in depression is calculated by the sucrose preference test. To perform this test, two containers, one containing water and the other containing 2% sucrose, were used. To reduce the stress response to the new conditions, the mice were allowed to freely choose between two bottles for drinking 24 hours before the test. During 3 days of the test, mice were free to choose one of the bottles (water or sucrose solution) to drink. During this period, the water container and sucrose were changed every 12 hours to prevent the possibility of errors in the test. The bottles were weighed at the beginning and end of period to calculate their consumption, and at the end of the third day, the ratio of sucrose to total consumption is measured. Depressed mice are less prone to sucrose [84].

5.1.2. Tail suspension test (TST)

Anhedonia and reduced motivation are core symptoms of depression. Anhedonia is known by an inability to experience pleasure and motivation. Both functions are mediated by over-lapping mesolimbic-striatal-cortical circuitry by activation of DA neurons in the VTA for processing and anticipating rewards [85,86]. In the case of the tail suspension test (TST) the stressful situation involves the haemodynamic stress of being hung to measure the tendency to despair. In this method, the mouse is hung in a box from the tail. Usually, after being hung, healthy mice start trying and paddling to escape and overcome their upset situation for at least 10 minutes. Mice under inescapable stress of being suspended become immobile; the duration of immobility is registered. Immobility is the relevant measure of behavioral despair. They will have some effort and consequently immobility while depressed animals will try less to escape the suspension and as a result, it will be immobile, so they will stop trying after about 2 to 4 minutes. During the experiment, which is 6 minutes, the immobility of the mouse was recorded [44].

5.2. Motor behavior

5.2.1. Open field test

Alterations of anxiety and exploratory of animals were evaluated by allowing mice to freely explore an open field arena for 5 min. The testing apparatus was a classic open field (i.e., a polyvinyl chloride square arena, 50×50 cm, with walls 40 cm high), surmounted by a video camera connected to a computer. Parameters such as time-spent locomotion, distance traveled, rearing (standing on hind legs) and grooming (licking, scratching, and face washing) were measured in 5 minutes. Total distance moved (TDM, cm); total duration mobility (s) and velocity (cm/s) were recorded for each mouse. At the end of each trial, the arena was cleaned with a 70% ethylic alcohol [87].

5.2.2. Rotarod test

To test the motor coordination and balance skills we used accelerating rotarod. All animals were pre trained 24 h before the test. Then, at the beginning of the test, mice were placed on the horizontal plastic rod rotating at an initial speed of 5 rpm, and the rotational velocity of the rod was linearly to 30 rpm. For each mouse, 3 trials with 300-s cut off was performed by 5 min interatrial interval and the average of staying time on the rod in 3 trials was calculated [24].

5.2.3. Wire grip or grasping test

This test is done to assessment muscle strength and balance. Each mouse was hung vertically with its front legs on a horizontal steel wire 80 cm long and 7 mm in diameter. The length of time that mouse can hold itself was recorded in 3 trials, and between each trial, the animal was given 5 min rest and the falling latency was recorded with a stop watch for each mouse [88].

5.3. Cognitive behavior

5.3.1. Passive avoidance learning (PAL)

PAL task is a fear-aggravated test used to evaluate associative learning and memory in rodents. PAL was measured as the last behavioral test and evaluated through use of a shuttle box. The shuttle box apparatus consisted of a light and a dark compartment, connected by a guillotine door. In the training session, animals were individually placed in the light compartment for one minute. After that, the door was opened and the mouse was allowed to move into the preferred dark chamber. At that point, the door was closed, and a 0.5 mA foot electric shock was delivered through the grid floor for three seconds. After 30 min, the same test was conducted again, and if the mice did not enter the dark chamber by 300 s, the successful acquisition of passive avoidance response was recorded (shock number) and the number of allowable shocks was 5. In the retention trials, each mouse was placed into the light compartment. Measures of the step-through latency (STL) defined as the time to enter the dark compartment and the time in the dark compartment (TDC) were utilized as indices of memory performance with a cut off time of 300-s [89].

6. Brain Tissue Separation

Animals were sacrificed immediately after their last behavioral assessment. Sacrifice was done by rapid and careful decapitation, and their brains were rapidly removed and were stored in liquid nitrogen and refrigerated at −80°C for evaluation of the degree of tyrosine hydroxylase (TH) activity and total antioxidant capacity (TAC).

7. Biochemical Assay

7.1. Assay of tyrosine hydroxylase (TH) activity in the brain tissue

Tyrosine hydroxylase (TH) is a marker for DA activity and the lesion of midbrain DA neurons induced by 6-OHDA was evaluated via analyzing the magnitude of TH, a rate-limiting enzyme for DA synthesis and an indicator of DA depletion [90]. Since midbrain neurons fibers reach the striatum and constitute the nigrostriatal DA system, it is markedly affected by exposure to 6-OHDA lesion. TH activity was assessed according to the manufacturer's instructions. First 10 mg midbrain tissue was weighted and

homogenized with a specific proportion of hydrolyzing solution and then centrifuged (12000rpm for 10 min). The 50 µl supernatant and 50 µl standard solution transferred to the ELISA plate with a multichannel pipette and were placed in a 96-well tissue culture plate on ice then 50 µl conjugate solution was added to them. The contents were incubated for 45 min in the room temperature after that the plate was washed five times. The amount of 100 µl of substrate was supplied to all the wells and after 10 min incubation in the room temperature. Finally, 50 µl of stop solution was added to stop the reaction, which will then turn the solution yellow. Absorbance was read at 540 nm using microplate reader and final values were calculated from protein standard curves. The intensity of the color directly proportional to the TH concentration. Protein standard curves were prepared and standard curve was blotted relating the intensity of the color (optical density =OD) to the concentration of standard. The TH concentration in each sample was interpreted from this standard curve. Finally, TH concentration was presented based on pg/ml.

7.2. Assay of total antioxidant capacity (TAC) in the brain tissue

Total Antioxidant Capacity (TAC) was rated according to the manufacturer's instructions using (Kiazist, Iran). In the CUPRAC method [91], copper (Cu + 2) is reduced to copper (Cu + 1) in the presence of antioxidants and produces color in the presence of chromogen. This color is absorbed at 450 nm. The oxidation of ferrous ions to ferric ions, which are correlated to the number of oxidant species at acidic pH, was used to assess the TOS in the brain homogenate. The iron (III) ion content was determined by xylenol orange.

8. Whole-cell Patch Clamp Recording (Wcr)

The effects of the CB1R agonist/antagonist on the electrophysiological properties of VTA DA neurons were evaluated by whole cell patch clamp in VTA brain slices of male mice (3 weeks). Animals were decapitated under diethyl ether anesthesia and brains were removed quickly. A block of the brain containing the VTA was incubated in ice-cold arti□cial cerebrospinal □uid (ACSF) containing (in mM) 124 NaCl, 25 NaHCO3, 10 D-glucose, 4.4 KCl, 2 MgCl2, 1.25 NaH2PO4 and 2 CaCl2, which was bubbled with 95% O2–5% CO2 (pH 7.4 ± 0.05 and osmolarity was adjusted to 300 ± 10 mOsm). The brain was then blocked in a coronal plane and sectioned at an interval of 250 µm thicknesses on a Vibroslicer (Campden Instrument, NVSLM1, Sarasota, FL, USA). The VTA area was visible in the fresh tissue as a gray region separated from the substantia nigra by white matter and located medial to the darker substantia nigra. Slices containing the VTA were incubated at 34 ± 2°C for 30 min and then stored at room temperature. The VTA slices were continuously superfused at 2 ml/min with ACSF. Whole cell patch clamp recordings in current clamp and voltage clamp modes were conducted from DA neurons which were identi□ed by well-established criteria de□ned below using a Multiclamp 700B ampli□er (Axon Instruments) and signals were digitized by a Digidata 1440 A/D converter (Axon Instruments). Electrophysiological records were sampled at 10 kHz and □ltered at 20 kHz, as described previously [25]. Patch pipettes had a resistance of 4–10 MΩ when □lled with internal solution containing (in mM) 140 potassium gluconate, 5 KCl, 10

HEPES, 2 MgCl2, 0.2 EGTA, 2 Na2ATP and 0.4 Na2GTP. The pH and the osmolarity of the internal solution were adjusted to 7.3 (by KOH) and 295 ± mOsm, respectively. VTA neurons were visualized with a 60× water immersion objective using Nomarski-type differential interference contrast (DIC) imaging with infrared illumination. After establishment of giga seal, brief suction was applied to break through the cell membrane for establishment of the whole cell configuration. Cells with a seal < 1 GΩ before rupture of the membrane were discarded and the test seal function was constantly employed and monitored throughout the recording to ensure that the seal was stable.

DA neurons can be distinguished from non-DA neurons by their electrophysiological characteristics. Only those neurons that were anatomically located within the VTA, and that conformed to the criteria for DA neurons (including slow spontaneous firing rate and presence of Ih currents) were studied. Putative VTA DA neurons were recognized by a prominent voltage sag caused by the hyperpolarization (−0.3 nA) activated cation current (Ih) in current-clamp mode and the presence of Ih in voltage clamp mode. Sag voltage in response to hyperpolarizing current pulses (100–500pA amplitude) was calculated as the peak voltage deflection divided by the amplitude of steady state voltage deflection using the following formula:

Sag voltage = Vpeak − Vsteady state

The number of action potentials generated in a rebound following negative current injection and the spike latency of the rst action potential were measured. In spontaneously ring neurons, action potential parameters including action potential half-width, action potential frequency and interspike interval were measured, as described previously [92]. To examine the effect of CB1R agonist/antagonist on Ih in VTA DA neurons, I-V activation curves were obtained in voltage clamp mode using 520 ms hyperpolarizing steps (50 to 140 mV; increment of 10 mV). The amplitude of Ih at each hyperpolarizing step was obtained by subtracting the instantaneous current amplitude from the steady-state current amplitude.

9. Drug Application

Drugs were applied in ACSF from a separate reservoir (also gassed with carbogen, 33–34 ^{o}C) to the recording chamber. 6-OHDA (hydrochloride salt; Sigma, USA) was dissolved in deionized water as a x100 stock solution containing 0.4% ascorbic acid. VTA DA cells exposed to ACSF (control) or 1 mM 6-OHDA (at least 20 min) [93] and WIN and AM were added to the bath in (2 μM) concentration [94].

10. Statistical Analysis

Statistical analysis and image production were performed using Graph Pad Prism (Graph Pad Software version 8, USA). Values are presented as the mean ± standard error. An unpaired Student t-test was used to compare behavioral results between control and mock groups. Normally distributed data were compared by two-way ANOVA and Tukey post hoc analysis was used for multiple comparisons between other groups. P <0.05 was considered statistically significant between groups.

Abbreviations

PD: Parkinson's disease, DA: Dopamine/ Dopaminergic, 6-OHDA: 6-hydroxydopamine, SNc: Substantia nigra pars compacta, SNr: Substantia nigra pars reticulata, ECBs: Endocannabinoid system, CB1R: Cannabinoid 1 receptor, BG: Basal ganglia, NMS: Non-motor symptoms, VTA: Ventral tegmental area, HCN: Hyperpolarization-activated cyclic nucleotide-gated channels, Ih: Hyperpolarization-activated current

Declarations

Author's contributions

Monavareh Soti contributed to study conception and design, acquisition of animal data, analyzing data, interpretation of the findings and writing the manuscript. Kristi Anne Kohlmeier, Hoda Ranjbar, Moazamehosadat Razavinasab, and Yaser Masoumi-Ardakani assisted with study conception and design, data analysis, interpretation of the findings and critical revision of the manuscript. Mohammad Shabani contributed to study conception and design, analyzing data, interpretation of the findings and writing the manuscript, and provided a critical revision of the manuscript for important intellectual content. All authors critically reviewed content and approved final version for publication.

Ethical statement

All experiments were done in accordance with the National Institutes of Health Guide for the Care and Use of Laboratory Animals (NIH Publication No. 80–23, revised 1996) and were approved by the Research and Ethics Committee of Kerman Universities of Medical Sciences, Kerman, Iran. The study is reported in accordance with **ARRIVE guidelines.**

Declaration of Competing Interest

The authors declare that they have no known competing financial interests or personal relationships that could have appeared to influence the work reported in this paper.

Data availability

All data generated or analysed during this study are included in this published article [and its supplementary information files].

Acknowledgement: Funding for this study was provided by Kerman University of Medical Sciences as a grant (97000860) for the PhD thesis conducted by Monavareh Soti.

Author Disclosures: All authors disclose any financial and personal relationships with other people or organizations that could inappropriately influence their work. All authors approve the final article.

References

1. De Lau, L. M. & Breteler, M. M. Epidemiology of Parkinson's disease. *The Lancet Neurology* **5**, 525–535 (2006).
2. Chen, J. J. Parkinson's disease: health-related quality of life, economic cost, and implications of early treatment. *The American journal of managed care* **16**, S87-93 (2010).
3. Chaudhuri, K. R. *et al.* The metric properties of a novel non-motor symptoms scale for Parkinson's disease: results from an international pilot study. *Movement disorders* **22**, 1901–1911 (2007).
4. Shulman, L., Taback, R. L., Rabinstein, A. & Weiner, W. J. Non-recognition of depression and other non-motor symptoms in Parkinson's disease. *Parkinsonism & related disorders* **8**, 193–197 (2002).
5. García-Arencibia, M., García, C. & Fernández-Ruiz, J. Cannabinoids and Parkinson's disease. *CNS & Neurological Disorders-Drug Targets (Formerly Current Drug Targets-CNS & Neurological Disorders)* **8**, 432–439 (2009).
6. Heo, J. Y. *et al.* Aberrant tonic inhibition of dopaminergic neuronal activity causes motor symptoms in animal models of Parkinson’s disease. *Current Biology* **30**, 276–291. e279 (2020).
7. Marsden, C. & Parkes, J. Success and problems of long-term levodopa therapy in Parkinson's disease. *The Lancet* **309**, 345–349 (1977).
8. Gerlach, M. *et al.* Dopamine receptor agonists in current clinical use: comparative dopamine receptor binding profiles defined in the human striatum. *Journal of neural transmission* **110**, 1119–1127 (2003).
9. Obeso, J. *et al.* The origin of motor fluctuations in Parkinson’s disease: importance of dopaminergic innervation and basal ganglia circuits. *Neurology* **62**, S17-S30 (2004).
10. Janvin, C. C. Cognitive impairment in patients with Parkinson’s disease: profiles and implications for prognosis. (2007).
11. Kulisevsky, J. *et al.* Acute effects of levodopa on neuropsychological performance in stable and fluctuating Parkinson's disease patients at different levodopa plasma levels. *Brain* **119**, 2121–2132 (1996).
12. Zou, S. & Kumar, U. Cannabinoid receptors and the endocannabinoid system: signaling and function in the central nervous system. *International journal of molecular sciences* **19**, 833 (2018).
13. Terzian, A. L., Drago, F., Wotjak, C. T. & Micale, V. The dopamine and cannabinoid interaction in the modulation of emotions and cognition: assessing the role of cannabinoid CB1 receptor in neurons expressing dopamine D1 receptors. *Frontiers in Behavioral Neuroscience* **5**, 49 (2011).
14. Howlett, A. *et al.* International Union of Pharmacology. XXVII. Classification of cannabinoid receptors. *Pharmacological reviews* **54**, 161–202 (2002).
15. Herkenham, M., Lynn, A. B., de Costa, B. R. & Richfield, E. K. Neuronal localization of cannabinoid receptors in the basal ganglia of the rat. *Brain research* **547**, 267–274 (1991).
16. Mailleux, P. & Vanderhaeghen, J.-J. Distribution of neuronal cannabinoid receptor in the adult rat brain: a comparative receptor binding radioautography and in situ hybridization histochemistry.

Neuroscience **48**, 655–668 (1992).

17. Weinstein, A. *et al.* A study investigating the acute dose—response effects of 13 mg and 17 mg Δ 9-tetrahydrocannabinol on cognitive—motor skills, subjective and autonomic measures in regular users of marijuana. *Journal of psychopharmacology* **22**, 441–451 (2008).
18. Romero, J. *et al.* The endogenous cannabinoid receptor ligand, anandamide, inhibits the motor behavior: role of nigrostriatal dopaminergic neurons. *Life sciences* **56**, 2033–2040 (1995).
19. Kreitzer, A. C. & Malenka, R. C. Endocannabinoid-mediated rescue of striatal LTD and motor deficits in Parkinson's disease models. *Nature* **445**, 643 (2007).
20. Jimenez-Del-Rio, M., Daza-Restrepo, A. & Velez-Pardo, C. The cannabinoid CP55, 940 prolongs survival and improves locomotor activity in Drosophila melanogaster against paraquat: implications in Parkinson's disease. *Neuroscience research* **61**, 404–411 (2008).
21. Chung, Y. C. *et al.* Cannabinoid receptor type 1 protects nigrostriatal dopaminergic neurons against MPTP neurotoxicity by inhibiting microglial activation. *The Journal of Immunology* **187**, 6508–6517 (2011).
22. Barzegar, S. *et al.* Effects of cannabinoid and glutamate receptor antagonists and their interactions on learning and memory in male rats. *Pharmacology Biochemistry and Behavior* **131**, 87–90 (2015).
23. Razavinasab, M. *et al.* Pharmacological blockade of TRPV 1 receptors modulates the effects of 6-OHDA on motor and cognitive functions in a rat model of P arkinson's disease. *Fundamental & clinical pharmacology* **27**, 632–640 (2013).
24. Shabani, M., Haghani, M., Sheibani, V. & Janahmadi, M. Changes in motor and learning behaviors of rats prenatally exposed to WIN 55212-2, a cannabinoid receptor agonist. *Physiology and Pharmacology* **13**, 120–129 (2009).
25. Shabani, M., Hosseinmardi, N., Haghani, M., Shaibani, V. & Janahmadi, M. Maternal exposure to the CB1 cannabinoid agonist WIN 55212–2 produces robust changes in motor function and intrinsic electrophysiological properties of cerebellar Purkinje neurons in rat offspring. *Neuroscience* **172**, 139–152 (2011).
26. Zarrindast, M.-R., Kangarlu-Haghighi, K., Khalilzadeh, A. & Fazli-Tabaei, S. Influence of intracerebroventricular administration of cannabinergic drugs on morphine state-dependent memory in the step-down passive avoidance test. *Behavioural pharmacology* **17**, 231–237 (2006).
27. Shabani, M., Divsalar, K. & Janahmadi, M. Destructive effects of prenatal WIN 55212-2 exposure on central nervous system of neonatal rats. *Addiction & health* **4**, 9 (2012).
28. Hasanein, P. & Far, M. T. Effects of URB597 as an inhibitor of fatty acid amide hydrolase on WIN55, 212-2-induced learning and memory deficits in rats. *Pharmacology Biochemistry and Behavior* **131**, 130–135 (2015).
29. Maroso, M. *et al.* Cannabinoid control of learning and memory through HCN channels. *Neuron* **89**, 1059–1073 (2016).
30. Biel, M., Wahl-Schott, C., Michalakis, S. & Zong, X. Hyperpolarization-activated cation channels: from genes to function. *Physiological reviews* **89**, 847–885 (2009).

31. Leresche, N., Jassik-Gerschenfeld, D., Haby, M., Soltesz, I. & Crunelli, V. Pacemaker-like and other types of spontaneous membrane potential oscillations of thalamocortical cells. *Neuroscience letters* **113**, 72–77 (1990).
32. McCormick, D. A. & Huguenard, J. R. A model of the electrophysiological properties of thalamocortical relay neurons. *Journal of neurophysiology* **68**, 1384–1400 (1992).
33. Doan, T. N. & Kunze, D. L. Contribution of the hyperpolarization-activated current to the resting membrane potential of rat nodose sensory neurons. *The Journal of physiology* **514**, 125–138 (1999).
34. Ludwig, A. *et al.* Absence epilepsy and sinus dysrhythmia in mice lacking the pacemaker channel HCN2. *The EMBO journal* **22**, 216–224 (2003).
35. Magee, J. C. Dendritic hyperpolarization-activated currents modify the integrative properties of hippocampal CA1 pyramidal neurons. *Journal of Neuroscience* **18**, 7613–7624 (1998).
36. Williams, S. R. & Stuart, G. J. Site independence of EPSP time course is mediated by dendritic I h in neocortical pyramidal neurons. *Journal of neurophysiology* **83**, 3177–3182 (2000).
37. Beaumont, V., Zhong, N., Froemke, R. C., Ball, R. W. & Zucker, R. S. Temporal synaptic tagging by Ih activation and actin: involvement in long-term facilitation and cAMP-induced synaptic enhancement. *Neuron* **33**, 601–613 (2002).
38. Beaumont, V. & Zucker, R. S. Enhancement of synaptic transmission by cyclic AMP modulation of presynaptic I h channels. *Nature neuroscience* **3**, 133–141 (2000).
39. Mercuri, N., Bonci, A., Calabresi, P., Stefani, A. & Bernardi, G. Properties of the Hyperpolarization-activated Cation Current Ih in Rat Midbrain Dopaminergic Neurons. *European Journal of Neuroscience* **7**, 462–469 (1995).
40. Santoro, B. *et al.* Molecular and functional heterogeneity of hyperpolarization-activated pacemaker channels in the mouse CNS. *Journal of Neuroscience* **20**, 5264–5275 (2000).
41. Notomi, T. & Shigemoto, R. Immunohistochemical localization of Ih channel subunits, HCN1–4, in the rat brain. *Journal of Comparative Neurology* **471**, 241–276 (2004).
42. Chu, H.-y. & Zhen, X. Hyperpolarization-activated, cyclic nucleotide-gated (HCN) channels in the regulation of midbrain dopamine systems. *Acta Pharmacologica Sinica* **31**, 1036–1043 (2010).
43. Masi, A., Narducci, R., Landucci, E., Moroni, F. & Mannaioni, G. MPP+-dependent inhibition of Ih reduces spontaneous activity and enhances EPSP summation in nigral dopamine neurons. *British journal of pharmacology* **169**, 130–142 (2013).
44. Cryan, J. F., Mombereau, C. & Vassout, A. The tail suspension test as a model for assessing antidepressant activity: review of pharmacological and genetic studies in mice. *Neuroscience & Biobehavioral Reviews* **29**, 571–625 (2005).
45. Mailleux, P. & Vanderhaeghen, J. J. Dopaminergic Regulation of Cannabinoid Receptor mRNA Levels in the Rat Caudate-Plitamen: An In Situ Hybridization Study. *Journal of neurochemistry* **61**, 1705–1712 (1993).

46. Romero, J. *et al.* Unilateral 6-hydroxydopamine lesions of nigrostriatal dopaminergic neurons increased CB1 receptor mRNA levels in the caudate-putamen. *Life sciences* **66**, 485–494 (2000).
47. Van Laere, K. *et al.* Regional changes in type 1 cannabinoid receptor availability in Parkinson's disease in vivo. *Neurobiology of aging* **33**, 620. e621-620. e628 (2012).
48. Palumbo, A., Napolitano, A., Barone, P. & d'Ischia, M. Nitrite-and peroxide-dependent oxidation pathways of dopamine: 6-nitrodopamine and 6-hydroxydopamine formation as potential contributory mechanisms of oxidative stress-and nitric oxide-induced neurotoxicity in neuronal degeneration. *Chemical research in toxicology* **12**, 1213–1222 (1999).
49. Blum, D. *et al.* Molecular pathways involved in the neurotoxicity of 6-OHDA, dopamine and MPTP: contribution to the apoptotic theory in Parkinson's disease. *Progress in neurobiology* **65**, 135–172 (2001).
50. Zhang, W. *et al.* Aggregated α-synuclein activates microglia: a process leading to disease progression in Parkinson's disease. *The FASEB Journal* **19**, 533–542 (2005).
51. Tadaiesky, M. *et al.* Emotional, cognitive and neurochemical alterations in a premotor stage model of Parkinson's disease. *Neuroscience* **156**, 830–840 (2008).
52. Campos, F. L. *et al.* Rodent models of Parkinson's disease: beyond the motor symptomatology. *Frontiers in behavioral neuroscience* **7**, 175 (2013).
53. Beppe, G. J. *et al.* Memory-enhancing activities of the aqueous extract of Albizia adianthifolia leaves in the 6-hydroxydopamine-lesion rodent model of Parkinson's disease. *BMC complementary and alternative medicine* **14**, 1–11 (2014).
54. Rodríguez de Fonseca, F. *et al.* The endocannabinoid system: physiology and pharmacology. *Alcohol and Alcoholism* **40**, 2–14 (2005).
55. Good, C. H. *et al.* Impaired nigrostriatal function precedes behavioral deficits in a genetic mitochondrial model of Parkinson's disease. *The FASEB journal* **25**, 1333–1344 (2011).
56. Chan, C. S. *et al.* HCN channelopathy in external globus pallidus neurons in models of Parkinson's disease. *Nature neuroscience* **14**, 85–92 (2011).
57. González, S. *et al.* Effects of rimonabant, a selective cannabinoid CB1 receptor antagonist, in a rat model of Parkinson's disease. *Brain research* **1073**, 209–219 (2006).
58. Kelsey, J., Harris, O. & Cassin, J. The CB1 antagonist rimonabant is adjunctively therapeutic as well as monotherapeutic in an animal model of Parkinson's disease. *Behavioural brain research* **203**, 304–307 (2009).
59. Di Marzo, V., Hill, M. P., Bisogno, T., Crossman, A. R. & Brotchie, J. M. Enhanced levels of endogenous cannabinoids in the globus pallidus are associated with a reduction in movement in an animal model of Parkinson's disease. *The FASEB Journal* **14**, 1432–1438 (2000).
60. El Banoua, F., Caraballo, I., Flores, J. A., Galan-Rodriguez, B. & Fernandez-Espejo, E. Effects on turning of microinjections into basal ganglia of D1 and D2 dopamine receptors agonists and the cannabinoid CB1 antagonist SR141716A in a rat Parkinson's model. *Neurobiology of disease* **16**, 377–385 (2004).

61. Janvin, C. C., Larsen, J. P., Aarsland, D. & Hugdahl, K. Subtypes of mild cognitive impairment in Parkinson's disease: progression to dementia. *Movement disorders: official journal of the Movement Disorder Society* **21**, 1343–1349 (2006).
62. Kumar, R., Agarwal, A. K. & Seth, P. K. Free radical-generated neurotoxicity of 6-hydroxydopamine. *Journal of neurochemistry* **64**, 1703–1707 (1995).
63. Lotharius, J., Dugan, L. L. & O'malley, K. L. Distinct mechanisms underlie neurotoxin-mediated cell death in cultured dopaminergic neurons. *Journal of Neuroscience* **19**, 1284–1293 (1999).
64. Ho, T. *et al.* A subpopulation of mesencephalic dopamine neurons projecting to limbic areas contains a cholecystokinin-like peptide: evidence from immunohistochemistry combined with retrograde tracing. *Neuroscience* **5**, 2093–2124 (1980).
65. Swanson, L. The projections of the ventral tegmental area and adjacent regions: a combined fluorescent retrograde tracer and immunofluorescence study in the rat. *Brain research bulletin* **9**, 321–353 (1982).
66. Tzschentke, T. M. Pharmacology and behavioral pharmacology of the mesocortical dopamine system. *Progress in neurobiology* **63**, 241–320 (2001).
67. McDaid, J., McElvain, M. A. & Brodie, M. S. Ethanol effects on dopaminergic ventral tegmental area neurons during block of I h: involvement of barium-sensitive potassium currents. *Journal of neurophysiology* **100**, 1202–1210 (2008).
68. Chang, X., Wang, J., Jiang, H., Shi, L. & Xie, J. Hyperpolarization-activated cyclic nucleotide-gated channels: an emerging role in neurodegenerative diseases. *Frontiers in molecular neuroscience* **12**, 141 (2019).
69. Razavinasab, M., Sheibani, V., Kohlmeier, K. A., Nazeri, M. & Shabani, M. Hyperexcitability of VTA dopaminergic neurons in male offspring exposed to physical or psychological prenatal stress. *Progress in Neuro-Psychopharmacology and Biological Psychiatry* **101**, 109923 (2020).
70. Henry, D. J. & Chavkin, C. Activation of inwardly rectifying potassium channels (GIRK1) by co-expressed rat brain cannabinoid receptors in Xenopus oocytes. *Neuroscience letters* **186**, 91–94 (1995).
71. Mackie, K., Lai, Y., Westenbroek, R. & Mitchell, R. Cannabinoids activate an inwardly rectifying potassium conductance and inhibit Q-type calcium currents in AtT20 cells transfected with rat brain cannabinoid receptor. *Journal of Neuroscience* **15**, 6552–6561 (1995).
72. Schweitzer, P. Cannabinoids decrease the K+ M-current in hippocampal CA1 neurons. *Journal of Neuroscience* **20**, 51–58 (2000).
73. Huang, Z., Walker, M. C. & Shah, M. M. Loss of dendritic HCN1 subunits enhances cortical excitability and epileptogenesis. *Journal of Neuroscience* **29**, 10979–10988 (2009).
74. Merrison-Hort, R. J. & Borisyuk, R. The emergence of two anti-phase oscillatory neural populations in a computational model of the Parkinsonian globus pallidus. *Frontiers in computational neuroscience* **7**, 173 (2013).

75. Hernández, M. *et al.* Cannabinoid CB1 receptors colocalize with tyrosine hydroxylase in cultured fetal mesencephalic neurons and their activation increases the levels of this enzyme. *Brain research* **857**, 56–65 (2000).
76. Szabo, B., Siemes, S. & Wallmichrath, I. SHORT COMMUNICATION Inhibition of GABAergic neurotransmission in the ventral tegmental area by cannabinoids. *European Journal of Neuroscience* **15**, 2057–2061 (2002).
77. Katona, I. *et al.* Distribution of CB1 cannabinoid receptors in the amygdala and their role in the control of GABAergic transmission. *Journal of Neuroscience* **21**, 9506–9518 (2001).
78. Wilson, R. I. & Nicoll, R. A. Endogenous cannabinoids mediate retrograde signalling at hippocampal synapses. *Nature* **410**, 588–592 (2001).
79. Wallmichrath, I. & Szabo, B. Cannabinoids inhibit striatonigral GABAergic neurotransmission in the mouse. *Neuroscience* **113**, 671–682 (2002).
80. Meurers, B. H. *et al.* Dopamine depletion induced up-regulation of HCN3 enhances rebound excitability of basal ganglia output neurons. *Neurobiol Dis* **34**, 178–188, doi:10.1016/j.nbd.2009.01.007 (2009).
81. Zheng, T. *et al.* CB1 cannabinoid receptor agonist mouse VD-hemopressin (α) produced supraspinal analgesic activity in the preclinical models of pain. *Brain research* **1680**, 155–164 (2018).
82. Ogawa, N. *et al.* Bromocriptine protects mice against 6-hydroxydopamine and scavenges hydroxyl free radicals in vitro. *Brain research* **657**, 207–213 (1994).
83. Chen, Y. *et al.* Brain gene expression of a sporadic (icv-STZ Mouse) and a familial mouse model (3xTg-AD mouse) of Alzheimer's disease. *PloS one* **7**, e51432 (2012).
84. Wang, S. *et al.* Anhedonia and activity deficits in rats: impact of post-stroke depression. *Journal of Psychopharmacology* **23**, 295–304 (2009).
85. Clark, D. A. & Beck, A. T. Cognitive theory and therapy of anxiety and depression: Convergence with neurobiological findings. *Trends in cognitive sciences* **14**, 418–424 (2010).
86. Holly, E. N. & Miczek, K. A. Ventral tegmental area dopamine revisited: effects of acute and repeated stress. *Psychopharmacology* **233**, 163–186 (2016).
87. Mohammadi, F., Esfahlani, M. A. & Shabani, M. Erythropoietin ameliorates harmaline-induced essential tremor and cognition disturbances. *Neuroscience letters* **704**, 153–158 (2019).
88. Golchin, L., Shabani, M., Harandi, S. & Razavinasab, M. Pistachio supplementation attenuates motor and cognition impairments induced by cisplatin or vincristine in rats. *Advanced biomedical research* **4**, 92, doi:10.4103/2277-9175.156656 (2015).
89. Razavinasab, M. *et al.* Early environmental enrichment prevents cognitive impairments and developing addictive behaviours in a mouse model of prenatal psychological and physical stress. *International journal of developmental neuroscience: the official journal of the International Society for Developmental Neuroscience*, doi:10.1002/jdn.10161 (2021).

90. Daubner, S. C., Le, T. & Wang, S. Tyrosine hydroxylase and regulation of dopamine synthesis. *Archives of biochemistry and biophysics* **508**, 1–12 (2011).
91. Apak, R., Güçlü, K., Özyürek, M. & Karademir, S. E. Novel total antioxidant capacity index for dietary polyphenols and vitamins C and E, using their cupric ion reducing capability in the presence of neocuproine: CUPRAC method. *Journal of agricultural and food chemistry* **52**, 7970–7981 (2004).
92. Haghani, M., Shabani, M., Javan, M., Motamedi, F. & Janahmadi, M. CB1 cannabinoid receptor activation rescues amyloid β-induced alterations in behaviour and intrinsic electrophysiological properties of rat hippocampal CA1 pyramidal neurones. *Cellular Physiology and Biochemistry* **29**, 391–406 (2012).
93. Berretta, N. *et al.* Acute effects of 6-hydroxydopamine on dopaminergic neurons of the rat substantia nigra pars compacta in vitro. *Neurotoxicology* **26**, 869–881 (2005).
94. Hajos, N. & Freund, T. Pharmacological separation of cannabinoid sensitive receptors on hippocampal excitatory and inhibitory fibers. *Neuropharmacology* **43**, 503–510 (2002).

Figures

Figure. 1

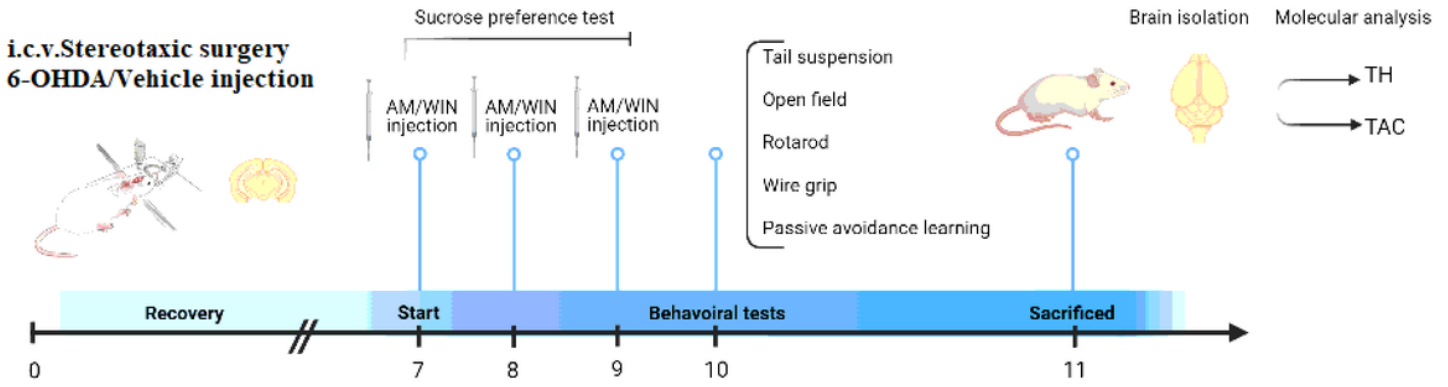

Figure 1

Behavioral experimental design

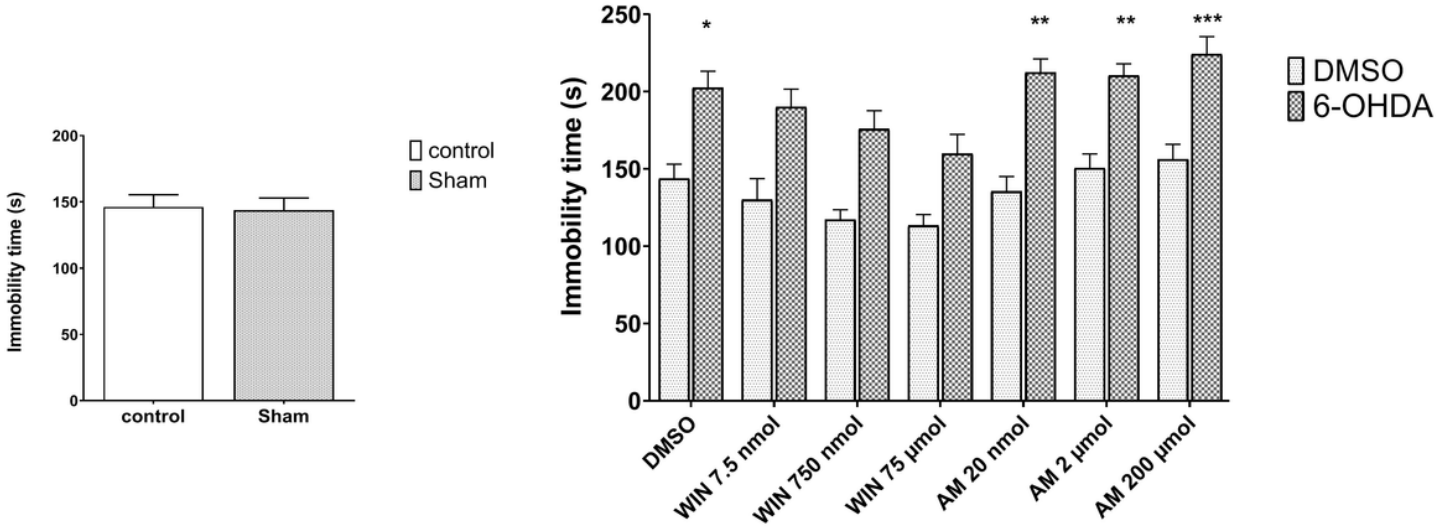

Figure 2

Behavioral despair evaluation of control, sham (DMSO) and 6-OHDA-treated mice in the tail suspension test. In these subsequent behavioral figures, an unpaired Student's t-test was used for comparisons of behavioral results between control and DMSO groups and there were no significant differences (panel A). A two-way ANOVA was used for comparisons of behavioral results between the DMSO and 6-OHDA treated animals who were treated with varying concentrations of CB1R agonist and antagonist (panel B). Results are shown as mean ± SEM (n=9). *P < 0.05, **P < 0.005, ***P < 0.001 versus DMSO.

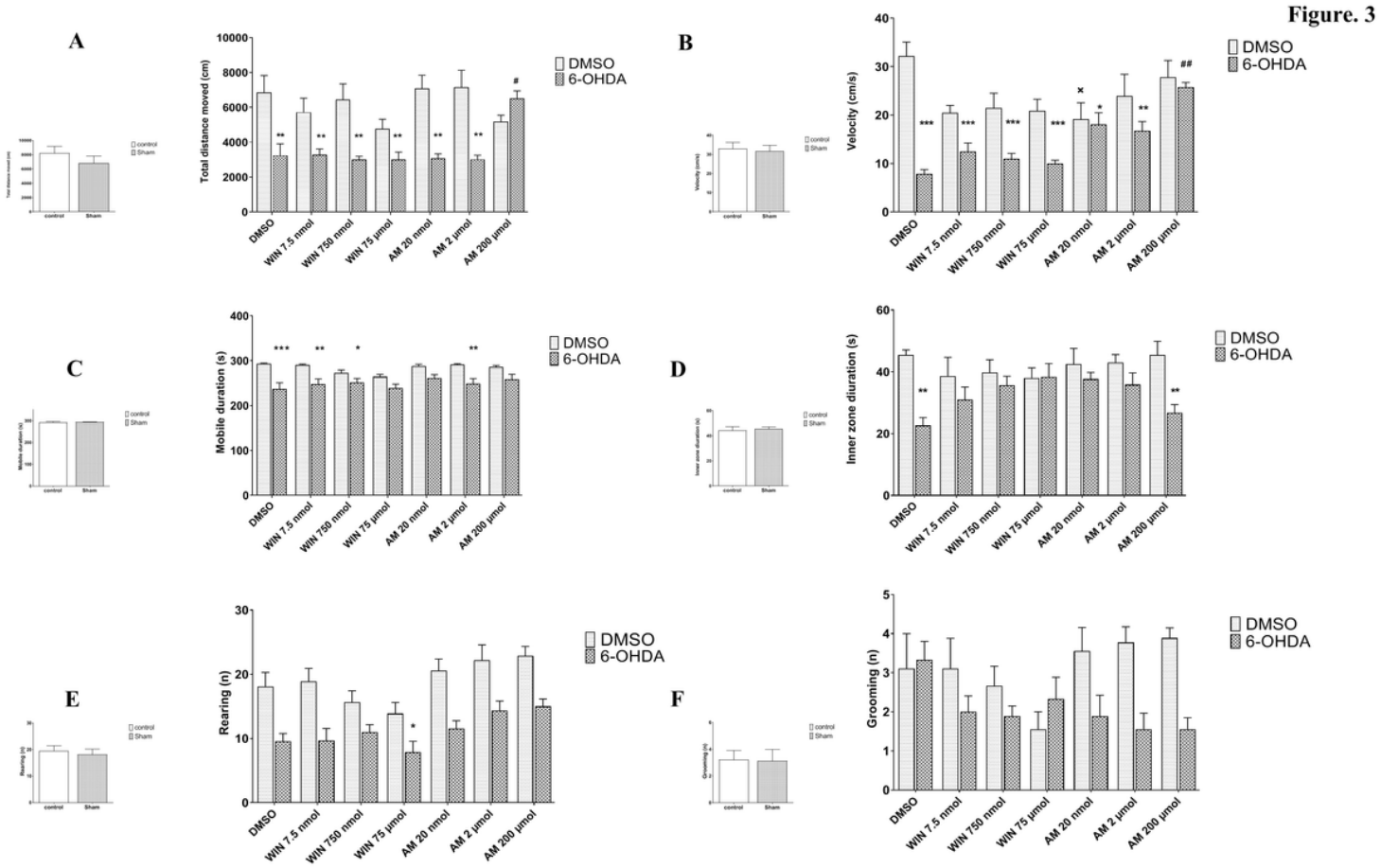

Figure 3

Characterization of exploratory activity and anxiety-related behaviors of control, DMSO and 6-OHDA treated mice in the open field test, 24 h after last injection. Results are shown as mean ± SEM (n=9). *P < 0.05, **P < 0.01, ***P < 0.001versus DMSO DMSO; #P < 0.05, ##P < 0.01, ###P < 0.001 versus 6-OHDA.

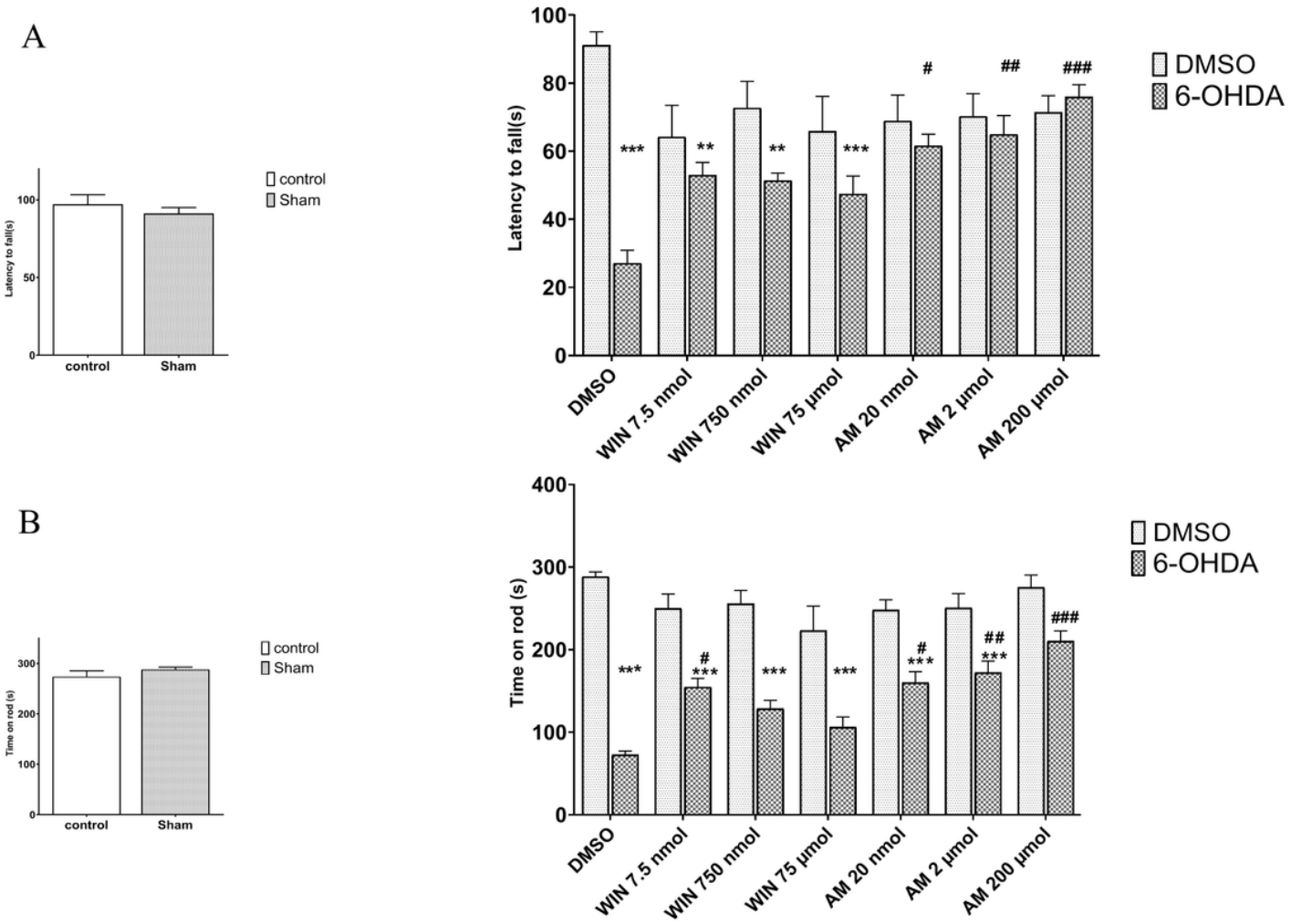

Figure 4

Motor coordination and balance function of healthy and PD mice in wire grip (A) and rotarod (B), 24h after last injection. Results are shown as mean ± SEM (n=9). *P < 0.05, **P < 0.005, ***P < 0.001 versus DMSO; #P < 0.05, ##P < 0.01, ###P < 0.001 versus 6-OHDA.

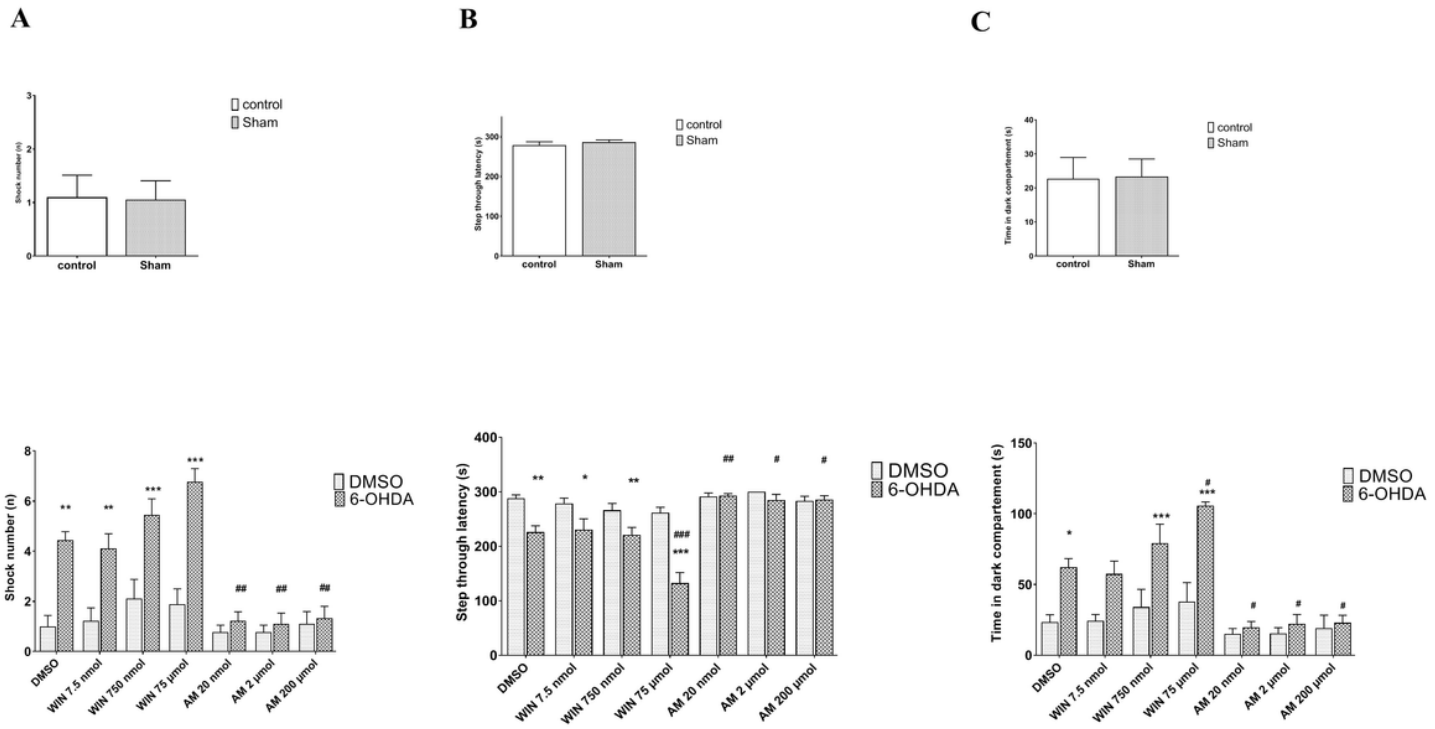

Figure 5

Passive avoidance memory analysis in control, DMSO and 6-OHDA-treated mice, 24 h after the last injection of the CB1R agonist/antagonist. Results are shown as mean ± SEM (n=9). *P < 0.05, **P < 0.01, ***P < 0.001versus DMSO; #P < 0.05, ##P < 0.01, ###P < 0.001 versus 6-OHDA.

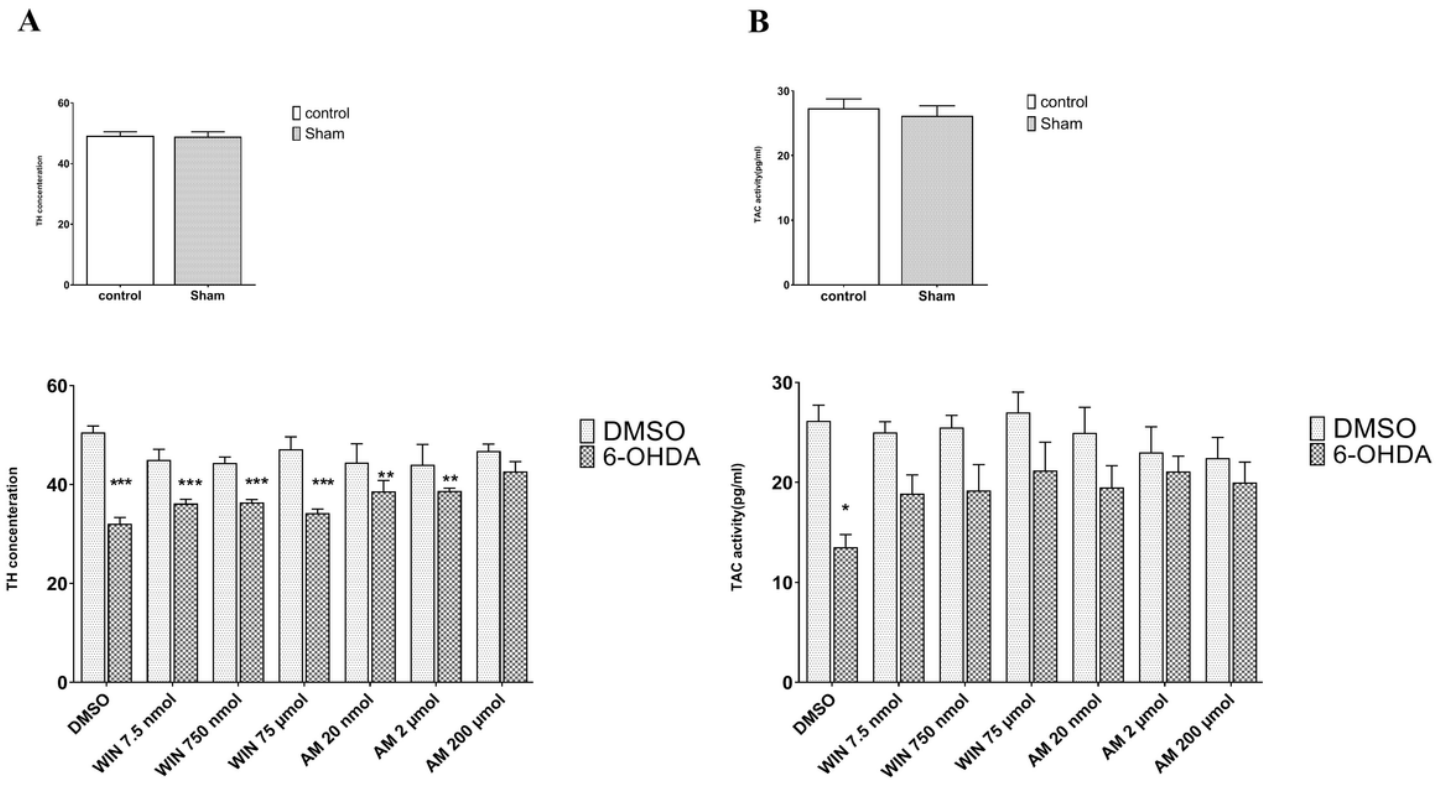

Figure 6

ELISA evaluated TH activity and TAC level in healthy and PD mice. Results are shown as mean ± SEM (n=9). *P < 0.05, **P < 0.01, ***P < 0.001 versus DMSO.

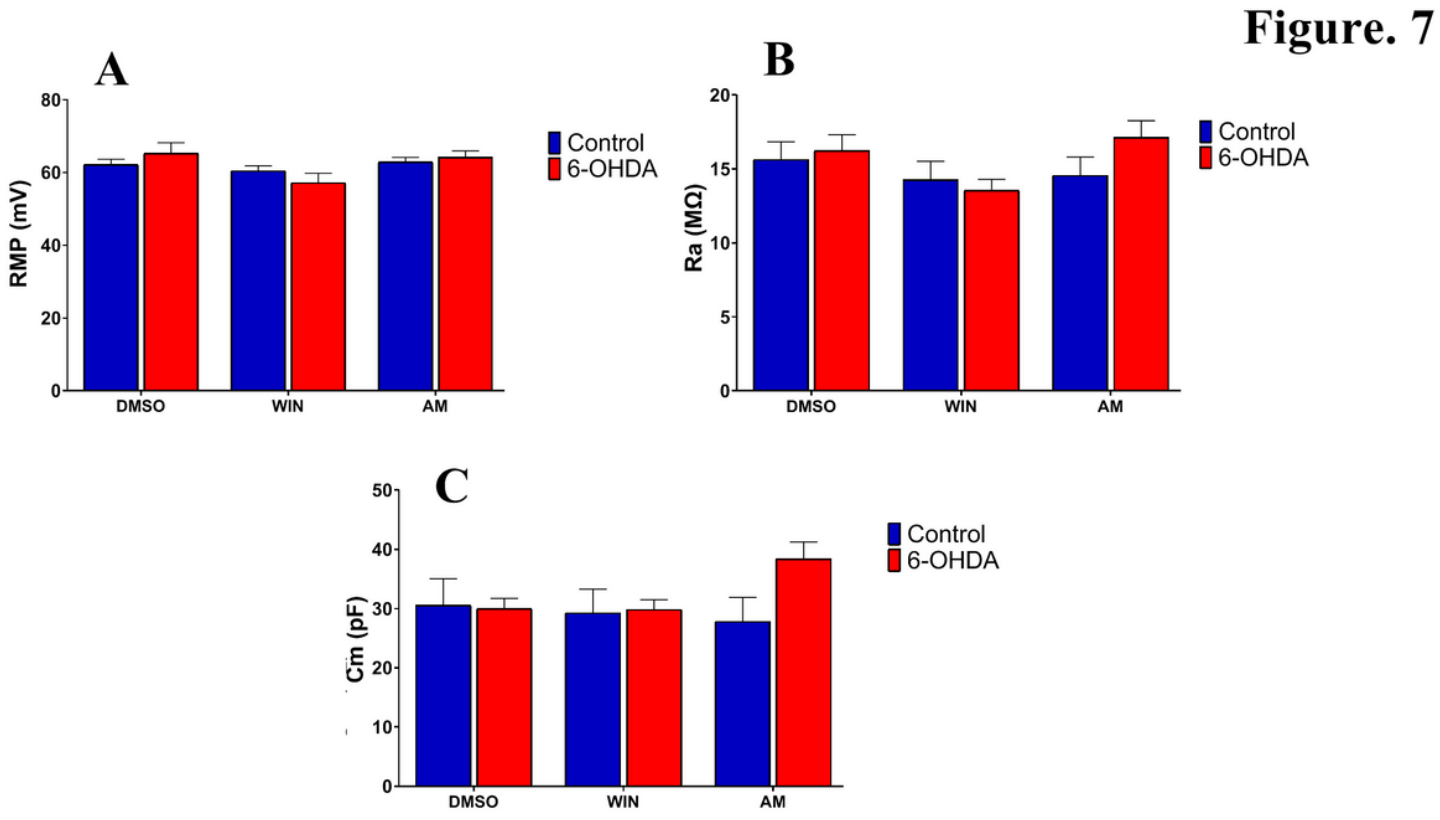

Figure 7

No significant differences were observed in passive properties (RMP, Ra and Cm) of VTA DA neurons following exposure to CB1R agonist/antagonist and 6-OHDA.

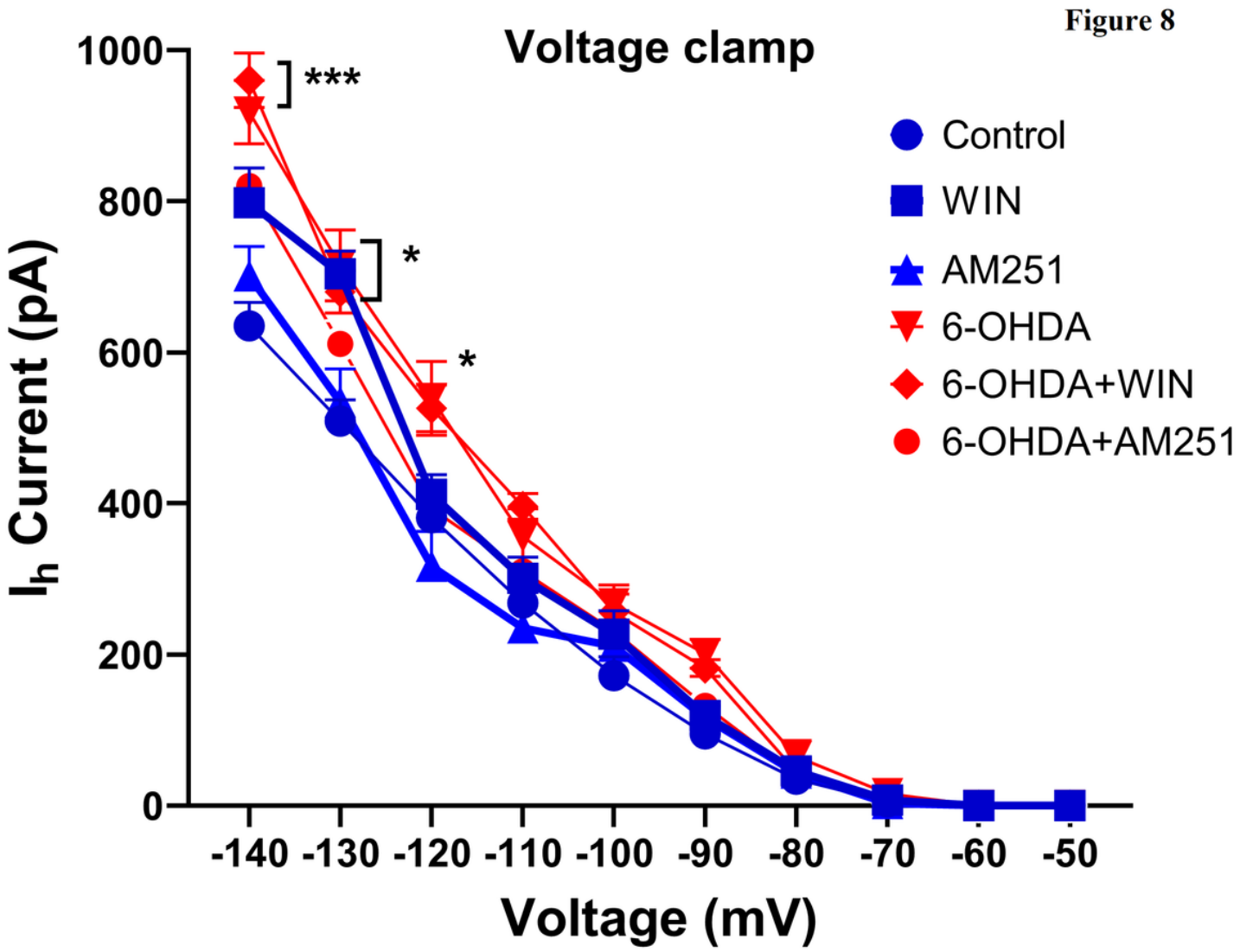

Figure 8

Changes in electrophysiological properties of VTA DA neurons of midbrain slices treated with CB1R agonist/antagonist and 6-OHDA. 6-OHDA alone and in combination with CB1R agonist resulted in an increase in the Ih currents at negative voltages of 120, 130 and 140 mV compared to control. The data are expressed as mean ± SEM. *($P < 0.05$), and*** ($P < 0.001$) represent the significant difference with the DMSO group.

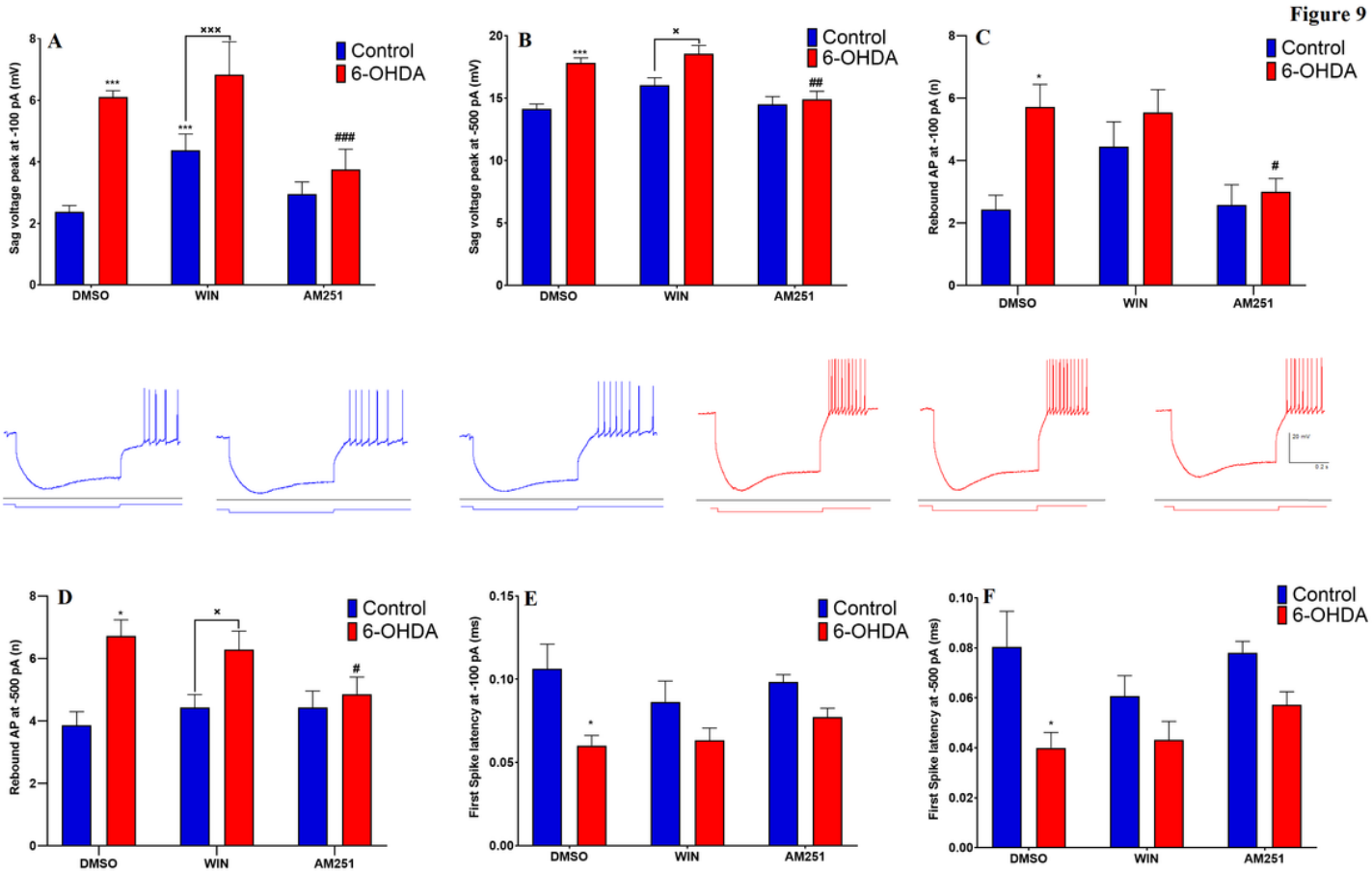

Figure 9

Electrophysiological properties of VTA DA neurons in slices exposed to CB1R agonist/antagonist in control and 6-OHDA treated slices. Sag voltage, rebound action potential firing, and first spike latency alternations in response to two fixed amplitude (−0.1 and 0.5 nA) injections of negative current are shown. Representative traces of sag voltage recorded from control and CB1R agonist/antagonist are depicted. The data are expressed as mean ± SEM. *($P < 0.05$) and represent a significant difference with the control (DMSO) group, and ($P < 0.05$), represent a significant difference with the WIN treated group. # ($P < 0.05$), represents the significant difference versus AM.

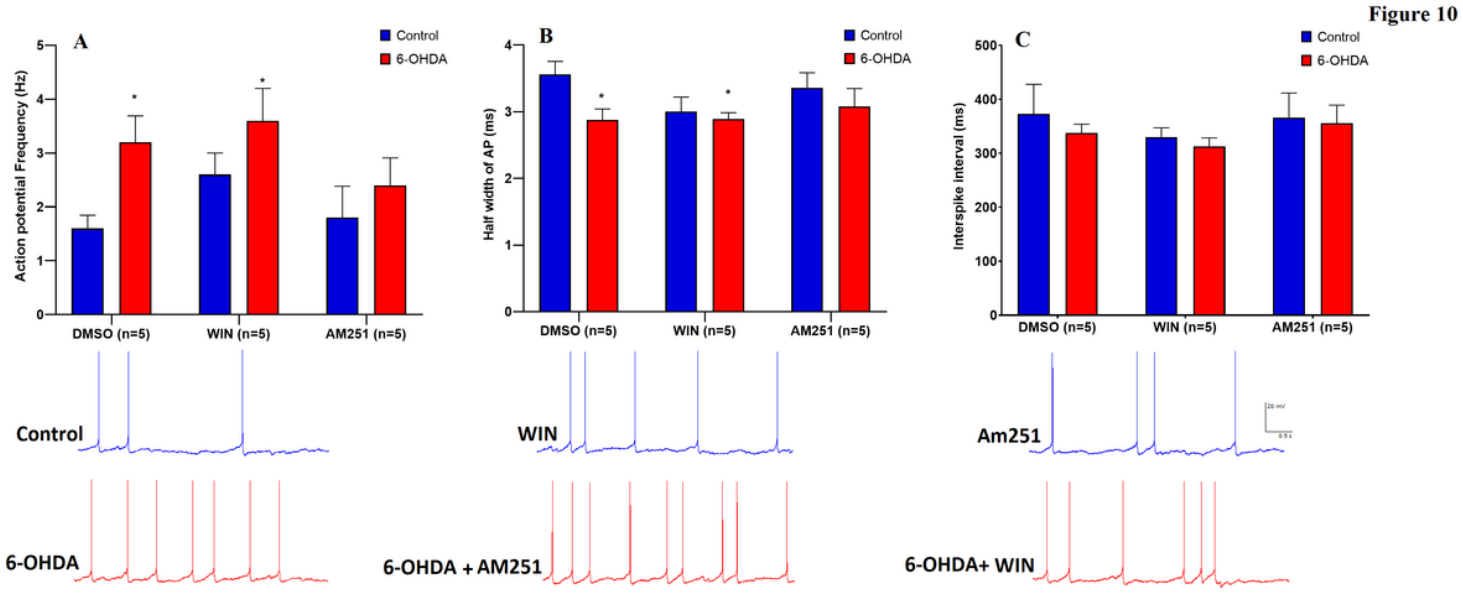

Figure 10

The effect of CB1R agonist/antagonist on the spontaneous firing properties of VTA DA neurons in control and 6-OHDA treated slices (A-C). Electrophysiological properties including, action potential frequency (A), action potential half-width (B) and interspike interval (C). The data are expressed as mean ± SEM. *(P < 0.05), represent the significant difference with the control (DMSO) group.

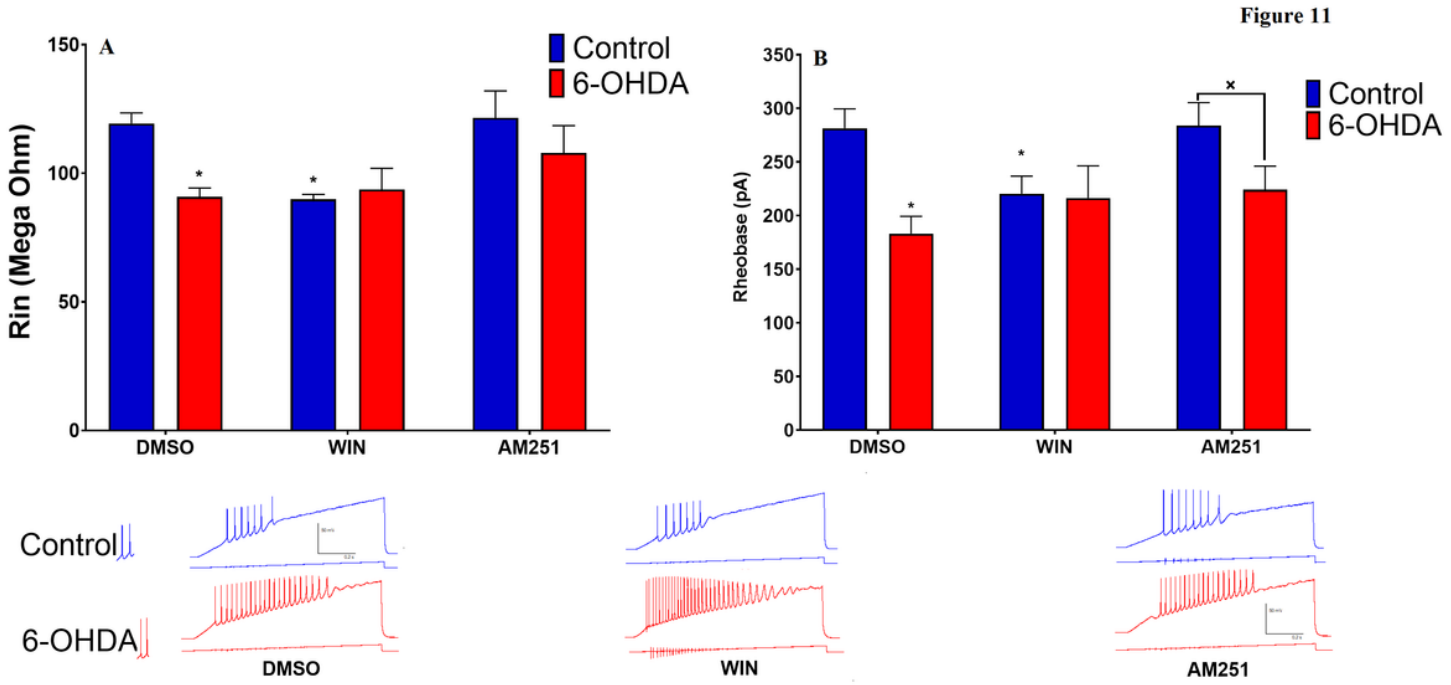

Figure 11

Rin and rheobase [the amount of current required to elicit an action potential] in response to ramp injected currents decreased in 6-OHDA and WIN groups. The data are expressed as mean ± SEM. *(P < 0.05), represent the significant difference with the control (DMSO), and x (P < 0.05), represent the significant difference with the WIN group.

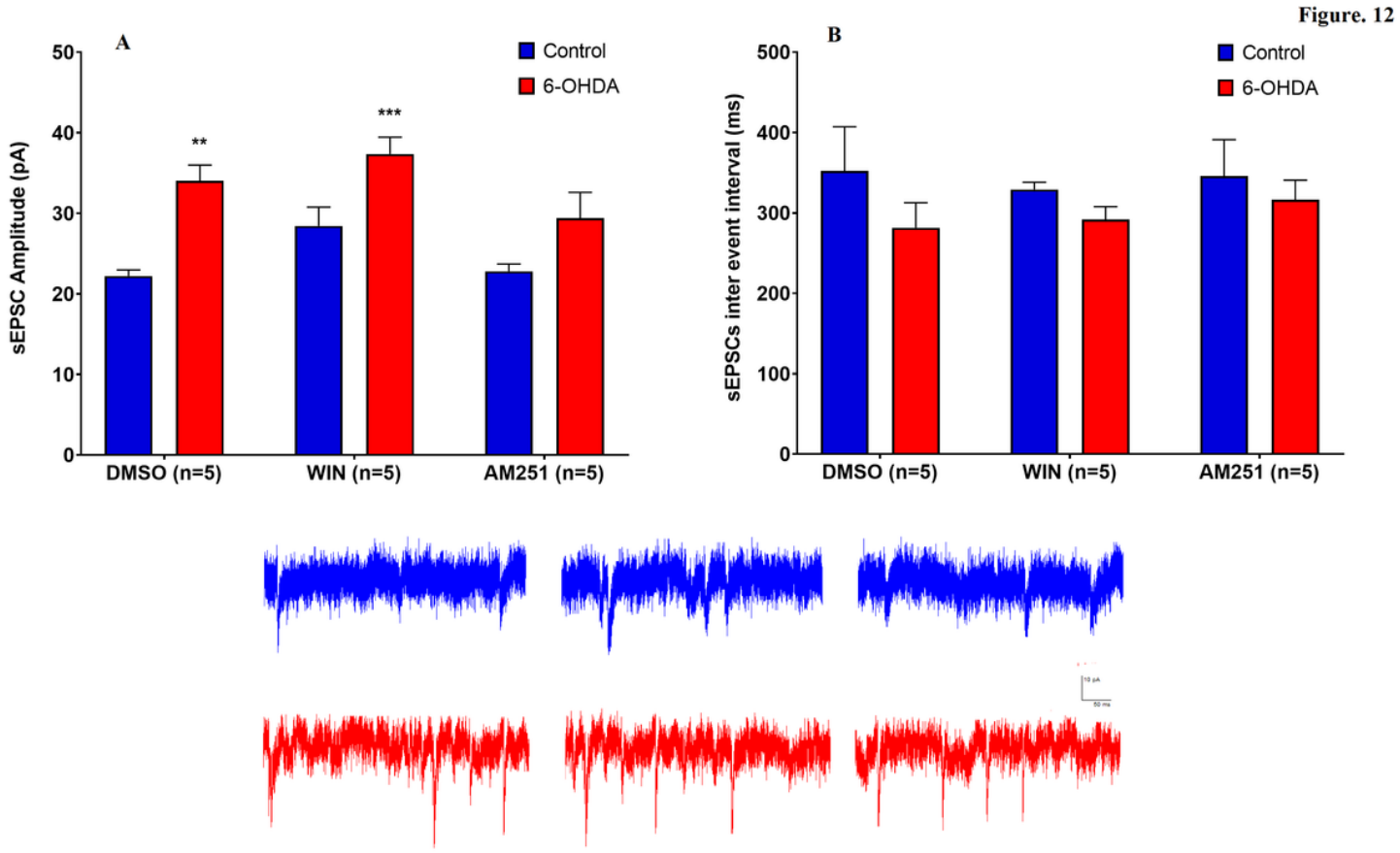

Figure 12

Representative the mean amplitude (A) and inter event interval (B) of sEPSCs in voltage clamp mode. Amplitude of sEPSCs is enhanced in both 6-OHDA and 6-OHDA+WIN groups. The data are expressed as mean ± SEM. ** (P < 0.01) and *** (P < 0.001) represent the significant difference with the control (DMSO) group.